NOX

RESULTS OF ABLATION TESTS ON SEVERAL PLASTIC MODELS IN A HYPERSONIC WIND TUNNEL

CONSTANTINO ECONOMOS

POLYTECHNIC INSTITUTE OF BROOKLYN

JULY 1961

AERONAUTICAL SYSTEMS DIVISION

RESULTS OF ABLATION TESTS
ON SEVERAL PLASTIC MODELS
IN A HYPERSONIC WIND TUNNEL

CONSTANTINO ECONOMOS

POLYTECHNIC INSTITUTE OF BROOKLYN

JULY 1961

FOREWORD

WADD TN 60-273

ABSTRACT

An experimental study of transient ablation has been carried out in a facility developed expressly for this purpose. The facility utilizes the PIBAL pebble bed convection heater as a source of high energy air.

Hemispherical models made of several plastic materials have been ablated in this facility and the final configuration compared with the predictions of a transient theory, which uses an integral technique. Good agreement has been found only for those plastics which may be classified as of a subliming type. For the remaining materials which melt and flow without significant vaporization the transient theory predicts values of the surface recession which are much lower than those obtained experimentally. This discrepancy many be attributable to unrealistic values of the physical properties available for these latter materials.

The models were exposed to both a laminar and transitional heat transfer environment. The appropriate heat transfer theories required for the calculation are reviewed and discussed in detail. Corresponding heating rates have been measured experimentally and are compared with these analyses. Theory and experiment are shown to be in good agreement.

A description of the facility and its development is presented in this report. In addition, a survey of current ablation theories is included in the introduction.

PUBLICATION REVIEW

This report has been reviewed and is approved.

FOR THE COMMANDER:
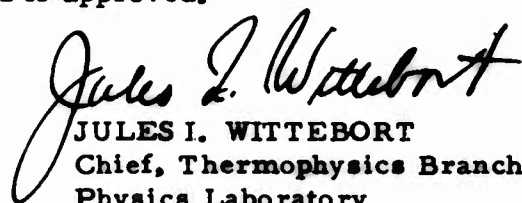
JULES I. WITTEBORT
Chief, Thermophysics Branch
Physics Laboratory
Directorate of Materials and Processes

TABLE OF CONTENTS

LIST OF FIGURES

LIST OF FIGURES (Contd)

LIST OF TABLES

LIST OF SYMBOLS

a   exponent in Eq. (42)

A   quantity defined by Eq. (29)

B   steady-state ablation velocity (in/sec)

c_f $2\tau_w / \rho_e u_e^2$ - local skin friction coefficient

c_p specific heat (Btu/lb.^{0}R)

C   quantity defined by Eq. (29)

D   quantity defined by Eq. (30)

F   function of $\overline{s}$ defined by Eq. (38)

G   quantity defined by Eq. (46)

h   film coefficient [Eq. (5)]

h   enthalpy (Btu/lb.)

h_c heat of combustion per unit mass of oxygen (Btu/lb. O_2)

h_{eff} effective heat of ablation (Btu/lb.)

k   thermal conductivity (Btu/in. sec.^{0}R)

K   quantity defined by Eq. (42)

L   heat of sublimation (Btu/lb.)

M   ratio of molecular weight of air to the injected vapor

m   steady-state mass rate of ablation (lb./in.^{2} sec.)

n   coordinate normal to wall

N_R $\rho_{t_e} \sqrt{h_{t_e}} \, R_o / \mu_{t_e}$ - Reynolds number

N_{R_ϑ}	$\rho_e u_e \vartheta / \mu_e$ - Reynolds number based on momentum thickness
Nu	$h \sqrt{\varkappa t}/k$ - transformed time coordinate
N_{Nu}	$q_w c_{p_t} R_o / k_{t_e} (h_{t_e} - h_w)$ - Nusselt number
p	pressure (lb./in.^{2})
q	net heat transfer rate to ablating surface (Btu/ft.^{2} sec.)
q_c	$\dfrac{0.21 h_c}{h_\infty - h_s}$ - combustion parameter
q_o	heat transfer rate to non-ablating surface (Btu/ft.^{2} sec.)
q_r	heat radiated from ablating surface (Btu/ft.^{2} sec.)
Q	heat stored in solid (Btu per unit area)
r	radial distance from axis of symmetry (in.)
R_o	radius of spherical nose (in.)
$\bar{r}$	r/R_o - nondimensional radius
s	location of vaporization line (in.)
s_t	$s(t_t)$ final location of vaporization line
S	distance along surface measured from stagnation point
$\bar{s}$	S/R_o - nomdimensional surface coordinate
t	time
t_t	total running time for ablation tests
T	temperature
u	velocity

$\bar{u}$	$u_e/\sqrt{h_{t_e}}$ - velocity ratio
V	$(T_s - T_i)$ - maximum temperature difference
x	space coordinate, one-dimensional semi-infinite slab
x'	transformed space coordinate $x - Bt + C$
x_0	initial depth of thermocouples (ablating models)
X	$x/2\sqrt{\varkappa t}$ - transformed space coordinate
Γ	gasification ratio
δ	e-folding length
ζ	$kV/q_0\delta$ nondimensionalized e-folding length
η	$q_0 s/kV$ nondimensional location of vaporization line
ϑ	momentum thickness
$\varkappa$	thermal diffusivity
λ	$kV/\varkappa(\rho L + H)$ - enthalpy ratio
μ	coefficient of viscosity
$\bar{\mu}$	μ_e/μ_{t_e} - viscosity ratio
Π	$2/3\,M^{\frac{1}{4}}\,\rho(h_\infty - h_s)$ - injection parameter
ρ	density
$\bar{\rho}$	ρ_e/ρ_{t_e} - density ratio
τ	$\varkappa(q_0/kV)^2 (t - t_s)$ nondimensional time
τ_w	wall shearing stress

Subscripts

e	conditions external to the boundary layer
i	initial conditions (prior to heating)
m	conditions evaluated at melting temperature
s	conditions evaluated at sublimation temperature
ss	steady-state conditions
t	stagnation conditions on model
w	wall conditions
∞	free-stream conditions

I. INTRODUCTION

A. Definition and Description of the Ablation Phenomenon

The interaction between the earth's atmosphere and a solid body traveling at hypersonic speeds has been studied for many years. Long before the first V-2 rocket was launched, astrophysicists (references 1 and 2) were concerned with this problem in connection with meteors. Recently, the aerodynamic heating problems associated with the reentry of ballistic missiles, satellites, and space vehicles, and with high performance propulsive systems have intensified the investigation of this interaction. A variety of heat protection systems have been developed for reentering vehicles. It is interesting that one of the most currently popular methods, namely that of ablation, bears a strong resemblance to the meteor problem studied in the past.

In its most general form the ablation phenomenon occurring during reentry represents an exceedingly complex problem in mathematical physics. Its solution requires a study of inviscid hypersonic flow, the heterogeneous compressible boundary layer, heat conduction, chemical reactions, dissociation and ionization, thermal stress analysis, and radiation, as well as the dynamics necessary for predicting the trajectory of a given body with specific initial conditions. Depending on the point of view many of these aspects may be treated independently.

The discussion to be presented here will be somewhat simplified in form. Some aspects of the general problem will be completely ignored, as they properly belong to fields distinct from aerodynamics. Certain additional information necessary for the solution of the problem will tacitly be assumed known.* For purposes of this discussion, consider the stagnation region of a blunt solid body suddenly exposed to a high energy

---

* For example, the heat transfer rates to a non-ablating body of arbitrary shape are required for certain aspects of the development. This requirement alone represents a major difficulty and continues to be the subject of intensive study at the present time (see, for example, references 3 and 4).

Manuscript released for publication 24 February 1961 as a WADD Technical Note.

stream of air. Assume that the initial temperature within the body is uniform and that the material melts at an elevated temperature. Until the surface of the body reaches the melting temperature, the heat which diffuses to the surface will merely be conducted into the interior of the solid; during this initial phase of heating the boundary layer and heat conduction problems are uncoupled and may be treated independently. However, as soon as a phase change does occur there arises a coupling of the two problems, with a resulting increase in complexity.

As an example consider the case when the heating is sufficient to cause vaporization of the solid, with or without an intermediate liquid phase. In either case the injection of gaseous products into the boundary layer results in a profound change in its character, adding new constituents to the mixture, thickening the boundary layer and altering the concentration, velocity, and enthalpy profiles. In general the result of this mass transfer is a reduction of the heat transfer rates at the interface. Obviously, the degree to which the heat fluxes are reduced depends on the rates at which the gases are evolved and vice versa; hence the coupling between the two previously independent systems.

Many additional complications may arise when melting and mass transfer occur. For example, if both liquid and gaseous phases coexist, the percentage of liquid which vaporizes before it is swept away by aerodynamic stresses must be determined. Of course, considerable simplification is possible if the solid material has a unique and clearly defined melting and/or boiling temperature. However, there are materials (the glasses, for example) which are not really solids but rather supercooled liquids. Such materials have a very high viscosity even at elevated temperatures, so that no distinct transition from solid to liquid phase is observed. The temperature at the gas-liquid interface becomes another unknown, resulting in an interdependence of the aerodynamic and heat conduction problems. It may be noted that for such materials the surface temperatures may reach values high enough for a significant quantity of energy to be radiated from the surface. Evidently such radiation is desirable as an additional mechanism for relieving the unfavorable thermal environment to which the body is subjected, provided that excessive heat transfer to the inner surface of the heat shield does not result from the elevated surface temperature.

The gaseous products injected into the boundary layer may react chemically with the original constituents of the boundary layer. In general, such a reaction can be expected to be exothermic, resulting in an increase in the heating potential to which the surface is exposed. The chemical kinetics of the reaction must of course be known if its effect on the overall

process is to be quantitatively determined.

The phase changes which occur at the surface of the solid also influence to a great extent the manner in which the heat conduction problem in the interior of the solid must be treated. The presence of a liquid layer and the evolution of gases by evaporation (or sublimation) at the liquid-gas (or solid-gas) interface introduces a nonlinear character because of the presence of moving boundaries. Such problems are usually referred to as "Stefan-like" (reference 5); exact analytic solutions for them are in general not available.

The presence of a liquid film on the surface of the solid results in the possible removal of material by both the aerodynamic forces as mentioned previously and by body forces which can arise from rapid decelerations of reentry bodies. In this connection the work of Cheng (reference 6) may be cited. It is demonstrated therein that rapid deceleration can result in an unstable liquid-gas interface which leads to a direct loss of mass as liquid droplets.

B. Review of Theoretical Works on Ablation

The theoretical treatment of the exceedingly complex ablation phenomenon requires a considerable idealization of the actual physical situation. In general, the analyses which have been performed are concerned with the simplified case of a stagnation region on blunt, two-dimensional or axisymmetric bodies. Such an approach permits the assumption of laminar flow and, of course, gives the boundary layer equations the "similar" character so essential to their solution.

For purposes of discussion, ablation may be categorized as occurring with melting only, with sublimation directly from the solid, or with a combination of melting and evaporation. In addition, one may consider alternately the cases where the gaseous products either react with the constituents of the external flow or are chemically inert.

An early work which studies the case of melting ablation is by Landau (reference 7) who assumed total, instantaneous removal of the ablated material under the condition of a constant heat input at the surface. Hence this study does not consider the interaction of the ablation products with the external boundary layer and is essentially a problem in heat conduction. The theory predicts the melting rate and the thickness of melted material as functions of time.

Goodman (reference 8) has considered the condition under which the assumption of instantaneous removal of the decomposition products is valid and has shown inter alia that the solid region must be semi-infinite in extent and that its surface temperature be held constant at its melting value.

Citron (reference 9) has carried out a similar analysis for the case of a finite solid region insulated at the unheated surface and has indicated that the treatments of Landau and the related work of Goodman cited above, and of Sutton (reference 10) yield melting rates which are too low.

Sutton presented one of the first rigorous analyses of melting ablation and its effect on the external boundary layer. Sutton has treated the case of Pyrex glass subjected to hypersonic flight conditions and integrated the liquid layer equations numerically. The importance of the viscosity of the molten material in blocking the heat conducted into the solid structure is pointed out.

Lees (reference 11) considered the case of melting ablation under the assumption of constant viscosity in the liquid layer and obtained approximate analytic solutions valid around body contours up to the sonic point. It was also shown herein that the stagnation enthalpy of the free-stream gas is an essential parameter which must be reproduced in experimental work if similitude is to be achieved.

Bethe and Adams (reference 12) treat the ablation of a glassy material (i.e., one with an exponential variation of viscosity with temperature) at a stagnation region, and consider the effect of partial vaporization of the molten film. There are obtained approximate solutions which determine the energy absorbed per unit mass of ablated material. In addition, the dependence of this and other ablation parameters on flight conditions is established.

The case of subliming ablation, which occurs with some plastic materials, is particularly well suited to treatment by a simplified engineering approach. Typically, it is assumed that the material has a unique sublimation or ablation temperature which is constant, that the phenomenon is quasi-steady (i.e., ablation proceeds at a constant rate), and that the thermal conductivity is small, so that the thermal penetration into the solid is negligibly small. The work of Roberts (reference 13) and Georgiev, Hidalgo, and Adams (reference 14) can be cited in this connection. The concept of the effective heat of ablation (h_{eff}) is utilized therein and estimates of its magnitude and its dependence on environmental conditions obtained by the analysis. Some experimental results are presented in

reference 14. Additional data may be found in references 15 and 16.

Much of the analysis of ablation with melting and evaporation has been carried out with reference to certain specialized types of materials. In particular, these are the glass-plastic combinations and the high-viscosity glasses such as quartz and Pyrex. The former materials, which may also be referred to as reinforced plastics, are produced by molding a mixture of a thermosetting plastic and refractory fibers (such as fiberglas), the plastic serving as the matrix for the reinforcing fibers. The concept of a gasification ratio Γ introduced by Scala (references 17 and 18) is useful in this case and represents an additional unknown of the problem.[*]

Typical of the theoretical and experimental investigations for a composite material is the work of Georgiev, Hidalgo, and Adams (reference 19) who consider the case of glass-reinforced phenolic plastic. It was found that the glass flowed without evaporation while the plastic matrix sublimed. The resulting interface temperature was shown to depend on the liquid flow, i.e., to be determined by the solution of the liquid layer equations. Additional work by Scala may be cited (reference 20) wherein a dependence of h_{eff} and Γ on stagnation pressure as well as on stagnation enthalpy is deduced.

Representative analyses for the glassy materials may be found in references 21 and 22. In the former a momentum integral technique is utilized for the determination of the steady-state ablation characteristics of the liquid layer. These equations, with assumed forms for the temperature and velocity distribution in the liquid regime, reduce to algebraic equations at the stagnation region. These are then matched with exact solutions for the dissociated gas phase (reference 23) to determine the various unknowns of the problem. Details of this procedure are given in reference 24. In reference 22, the identical problem is considered with the liquid assumed to be incompressible and with a temperature dependent viscosity. The governing equations are dedeuced and temperature, shear stresses, mass and energy transfer matched at the gas-liquid, liquid-solid interfaces. A numerical solution for Pyrex glass is presented.

An experimental and theoretical study in which the capabilities of the various types of ablation are compared, may be found in references 18 and 21. It is shown therein that the selection of the "best" material

---

[*]The gasification ratio Γ represents the fractional part of the solid which gasifies.

depends critically on flight conditions, that is, on the type of application intended. This latter aspect will be discussed briefly in the next section.

Mac C. Adams (reference 25), in an extensive and thorough survey article, presents correlation formulas for the effective heat of ablation for quartz and for a glass-plastic combination. These relations are based on the work performed in some of the aforementioned references (11, 19, and 26) and yield simple engineering formulas which relate h_{eff} to free-stream stagnation pressure and enthalpy. Estimates for the case of turbulent heating are also indicated.

Ablation with chemical reaction has been treated by several investigators (references 18, 27, and 28). In particular, the work of Knuth (reference 27) and Denison and Dooley (reference 28) will be outlined here as being representative. Any analysis of this problem requires rather detailed information concerning the chemical kinetics of the ablating material. In general, such information is not available for technologically interesting reactions so that at present quantitative results can only be obtained for a few materials. The references cited above consider the ablation (with combustion) of Teflon and graphite.

Knuth treated the steady Couette flow with diffusion of a reacting gas (the Teflon monomer C_2F_4). Under the assumption of infinitely fast (and infinitely slow) reaction rates the pertinent equations are deduced, and velocity, enthalpy, and partial pressure profiles calculated therefrom. An important result is that the ablation rate of Teflon when exposed to a hypersonic environment is influenced insignificantly by combustion of the monomer.

In reference 28, a detailed aerothermochemical analysis of chemically active surfaces in a high speed airstream of an oxidizing gas mixture is presented and applied to the particular case of graphite. In agreement with several other works (references 27, 29, and 30), it is shown that the exothermic reaction does not greatly affect the mass and heat transfer at the solid surface when the heating rate is sufficiently high to cause the reaction to occur within the boundary layer.

C. Engineering Significance and Applications of Ablation

The effectiveness of ablation in extreme thermochemical environments is most evident when it is compared with other methods of protection, such as the heat sink, radiators, and transpiration cooling. A comparison of these on a weight basis indicates that ablation is one form

or another (see previous remarks about various types of ablation) is the most practical and effective for virtually all of the aforementioned environmental conditions (see, for example, reference 17). Another advantage of the ablation is its passivity and the self-regulation which it exhibits; that is, as the heat transfer rate to the ablating surface increases, the rate of ablation increases so as to absorb the increase and to reduce the heat transfer rate. The practicability of the ablation process in missile applications has already been established.

D. Summary

The references cited above are representative of the effort devoted recently to the ablation phenomenon. Although a great part of this work utilizes a highly theoretical approach which yields a broader understanding of the underlying principles governing the process, it is interesting to note that the major contribution to the solution of the reentry problem has been due to research involving an elementary engineering point of view in combination with experiment. The major factor which distinguishes the two approaches is that in the latter case steady-state ablation is considered. It is evident, however, that in order to make final design estimates and to check the validity of these approximate calculations, the more complicated transient ablation analysis must be carried out. Consequently, experimental techniques for the study of the transient case must also be developed.

For materials of practical interest exposed to the high heat fluxes corresponding to typical reentry conditions, the accurate measurement of the transient behavior is exceedingly difficult, due to the relatively rapid rate with which the ablation becomes steady. One way by which this difficulty can be overcome is by exposing the models to air streams of relatively low stagnation enthalpies. In this way the transient portion of the process is extended in time so that accurate measurements may be obtained. If in addition the models are large, further precision results.

The facility and the experimental techniques which are described in this report were developed in keeping with this point of view. The wind tunnel used to ablate the models which were tested produces an airstream capable of ablating the specimens with a significant transient period; this permits a photographic resolution with time of the unsteady surface recession. The size of the models which were designed enhanced the precision of these measurements and also permitted the installation of thermocouples below the surface, so that additional data of interest could be obtained. In the next section the theoretical consideration required for the reduction of the data is presented. Then follows a description of the development of the

facility and the design of the models and test procedure utilized. Finally, the data whichhave been obtained are discussed and compared with the pertinent theories.

II. THEORETICAL ANALYSES

A. Transient Ablation

The transient sublimation of a semi-infinite, one-dimensional solid with constant physical properties, exposed to a hypersonic airstream with constant flow properties, is considered. In particular, it is assumed that the solid sublimes at a definite and unique temperature hereinafter referred to as the sublimation temperature and denoted by T_s. The analysis is generally specialized to the conditions under which the experimental portion of this investigation has been conducted.

The phenomenon of transient sublimation can be separated into three distinct time intervals, each involving a different mathematical description or analysis. These time intervals can be defined as

$$0 \leq t \leq t_s$$

$$t_s \leq t \leq t_{ss}$$

$$t_{ss} \leq t \leq \infty$$

where t_s is the time required for the surface of the solid material to reach the sublimation temperature T_s, and t_{ss} represents the time required to achieve a condition of steady state sublimation. Mathematically, this latter time is indistinguishable from $t \longrightarrow \infty$, but from a physical point of view this distinction is warranted, as will be seen below. The time $t=0$ corresponds to the instant of application of the heat flux.

Initially the solid is assumed to be at a uniform temperature $T_i (T_i < T_s)$. At $t=0$ it is instantaneously exposed to a hypersonic airstream

with steady flow properties. Until the surface of the solid reaches the temperature T_s, the solid can be considered to be an idealized heat sink with the temperature-time history described by the unsteady, one-dimensional heat conduction equation (see Fig. 1 for coordinate system)

$$\varkappa \frac{\partial^2 T(x,t)}{\partial x^2} = \frac{\partial T}{\partial t} \qquad 0 \le t \le t_s \qquad (1)$$

with initial condition

$$T(x,0) = T_i \qquad (2)$$

and boundary conditions

$$\lim_{x \to \infty} T(x,t) = T_i \qquad (3)$$

$$- k \frac{\partial T(0,t)}{\partial x} = h[T_\infty - T(0,t)] \qquad (4)$$

Here, $\varkappa$ and k represent the thermal diffusivity and conductivity of the solid, respectively, and h the heat transfer or film coefficient defined by the relation

$$h = \frac{q_o(t)}{T_\infty - T(0,t)} \qquad (5)$$

where q_o is the net heat flux per unit area to the surface x=0, and T_∞ is the stagnation temperature of the external flow. The film coefficient h is assumed to be constant in this analysis. The solution to the system (1)-(4) can be found in the literature (see, for example, reference 31) and is given by

$$T(x,t) = T_i + (T_\infty - T_i)\, [\mathrm{erfc}\, X - e^{Nu(Nu+2X)}\, \mathrm{erfc}\,(Nu+X)] \qquad (6)$$

FIG. 2 COMPARISON OF ASSUMED
AND EXACT TEMPERATURE PROFILES
MODEL T10 $\bar{s} = 0$

FIG. 1 COORDINATE SYSTEM
ABLATING SEMI-INFINITE SLAB

where

$$X = \frac{x}{2\sqrt{\varkappa t}} \quad , \qquad Nu = \frac{h\sqrt{\varkappa t}}{k} \tag{7}$$

the notation being that of reference 32.

The quantity t_s can now be evaluated from the relation

$$T(0,t_s) = T_s = T_i + (T_\infty - T_i)(1 - e^{Nu^2} \operatorname{erfc} Nu) \tag{8}$$

obtained by setting $X=0$ in Eq. (6). The temperature distribution at time $t=t_s$, namely $T(x,t_s)$, can then be obtained, again utilizing Eq. (6).

When the surface of the solid is at the sublimation temperature the solid will vaporize, and the vapor will be injected into the boundary layer, where it is removed by convection. The surface of the solid will recede. Let $x=s(t)$ denote the distance of this receding surface from its initial position $x=0$. Thus, $x=s(t)$ represents a moving interface between the solid material and the external gas boundary layer. If $q(t)$ is the net heat flux to this surface, L the heat of sublimation of the solid and ρ its density, an energy balance at the interface requires that

$$-k \frac{\partial T(s,t)}{\partial x} = q(t) - \rho L \frac{ds}{dt} \quad . \tag{9}$$

That is, the net heat flux to the solid is partly utilized to sublime some of the solid while the remainder is conducted into the interior.

For the process described above an unsteady heat conduction problem can be formulated as follows: for $s \leq x \leq \infty$ and $t_s \leq t$, the heat conduction Eq. (1) is valid and the following boundary conditions apply:

$$\lim_{x \longrightarrow \infty} \frac{\partial T(x,t)}{\partial x} = 0 \tag{10}$$

$$T(s,t) = T_s \qquad (11)$$

while the initial spatial temperature distribution is given by the constant
h analysis presented previously, namely:

$$T(x,t_s) \qquad (12)$$

The solution to the problem defined by the system of Eqs. (1), (10),
(11), and (12) presents considerable difficulty due to the existence of the
moving boundary s(t). A method analogous to the Karman and Polhausen
momentum integral (reference 33) can be used to satisfy the heat conduction
equation on the average and to obtain an approximate but simple solution.
The "heat-balance integral" thus obtained was introduced by Goodman
(reference 34) and applied to various heat conduction problems involving a
change of phase. Such a technique does not yield exact results, but simple
analytic solutions can be obtained which appear to have sufficient accuracy
for most engineering purposes.

The analysis presented below differs from that in reference 34 in
two important respects. First, in the choice of a temperature profile
within the solid, and second in the assumed form for the heat flux rate. In
particular, it may be noted that in the aforementioned reference $T(x,t)$ is
taken to be parabolic in form, while $q(t)$ is assumed to be constant. In
what follows these are replaced by Eqs. (13) and (14) which appear to be
somewhat more realistic. The justification for these particular choices is
discussed in Appendices I and II.

Let the temperature distribution within the unablated solid be given
by

$$T(x,t) = T_i + (T_s - T_i) \exp\left[-\frac{x-s(t)}{\delta(t)}\right] \qquad (13)$$

In addition let

$$q(t) = q_o - \Pi \frac{ds}{dt} \qquad (14)$$

where q_o and Π will depend only on the physical properties of the solid and
on free-stream conditions; their significance as well as that of the quantity

(t) introduced in Eq. (13) are discussed in the appendices.

Eq. (1) is now integrated over the remaining solid, i.e.:

$$\int_{s(t)}^{\infty} \varkappa \, \frac{\partial^2 T}{\partial x^2} \, dx = \int_{s(t)}^{\infty} \frac{\partial T}{\partial t} \, dx$$

from which

$$\varkappa \left[\frac{\partial T(\infty, t)}{\partial x} - \frac{\partial T(s, t)}{\partial x} \right] = \frac{d}{dt} \int_{s}^{\infty} T(x, t) \, dx + T(s, t) \, \frac{ds}{dt} \qquad (15)$$

From the boundary conditions (10) and (11) and the assumed profile (13), Eq. (15) becomes

$$\frac{\varkappa}{\delta} = \frac{d\delta}{dt} + \frac{ds}{dt} \qquad (16)$$

while (9) becomes [utilizing Eq. (14)]

$$\frac{kV}{\delta} = q_o - (\rho L + \Pi) \, \frac{ds}{dt} \qquad V \equiv (T_s - T_i) \qquad (17)$$

Eliminating ds/dt between Eqs. (16) and (17) there is obtained a differential equation for the quantity $\delta(t)$ as follows:

$$\frac{d\delta}{dt} - \frac{1}{\delta} \left[\varkappa + \frac{kV}{\rho L + \Pi} \right] + \frac{q_o}{\rho L + \Pi} = 0 \qquad (18)$$

Eqs. (17) and (18) represent two simultaneous, ordinary differential equations for δ and s. The initial conditions for this system are

$$\text{for} \quad t=t_s, \quad s=0, \quad \frac{ds}{dt} = 0 \implies \delta = \frac{kV}{q_o} \tag{19}$$

Introducing now the transformations

$$\tau = \varkappa \left(\frac{q_o}{kV}\right)^2 (t-t_s) $$

$$\eta = \frac{q_o}{kV} s \tag{20}$$

$$\zeta = \frac{kV}{q_o} \frac{1}{\delta}$$

$$\lambda = \frac{kV}{\varkappa(\rho L + \Pi)}$$

the systems (17) and (18) become

$$\frac{d\zeta}{d\tau} + (1+\lambda) \zeta^2 - \lambda \zeta^3 = 0 \tag{21}$$

$$\frac{d\eta}{d\tau} + \lambda \zeta - \lambda = 0 \tag{22}$$

and the initial conditions transform as

$$\tau = 0; \quad \eta = 0, \quad \zeta = 1 \tag{23}$$

The solution to this system is quite easily obtained. It is

$$\tau = \frac{1+\lambda}{\lambda^2} \ln\left[\frac{\zeta}{(1+\lambda)\zeta - \lambda}\right] - \frac{1}{\lambda} \left(\frac{1}{\zeta} - 1\right) \tag{24}$$

$$\eta = \frac{\lambda}{1+\lambda} \left[\tau - \left(\frac{1}{\zeta} - 1 \right) \right] \qquad (25)$$

for $\lambda \neq 0$. Note that for large times (i.e., $\tau \longrightarrow \infty$)

$$\zeta \longrightarrow \frac{\lambda}{1+\lambda}$$

$$(26)$$

$$\eta \longrightarrow \frac{\lambda}{1+\lambda} \tau - \frac{1}{1+\lambda}$$

These conditions represent the steady-state solution referred to previously; that is, for large times the ablation velocity is constant, as is the temperature distribution within the remaining solid; this may be verified by inspection of the temperature profile of Eq. (13) under the steady state requirements outlined in Eq. (26). The profile takes the form

$$\frac{T(x,t) - T_i}{T_s - T_i} = \exp[-A(x - Bt + C)] \qquad (27)$$

With respect to a coordinate system fixed with the steadily receding surface (i.e., with velocity B) the profiles have the form

$$\frac{T(x',t) - T_i}{T_s - T_i} = \exp(-Ax')$$

$$(28)$$

$$x' \equiv x - Bt + C$$

and so the profiles are time independent. The constants introduced above are defined by

$$A = \frac{B}{\varkappa}$$

$$B = \frac{\lambda}{1+\lambda} \frac{q_0 \varkappa}{kV} \quad \text{(the steady-state ablation velocity)} \qquad (29)$$

$$C = B\left[t_s + \left(\frac{kV}{q_0}\right)^2 \frac{1}{\lambda \varkappa}\right]$$

Eqs. (24) and (25) are plotted in Fig. 3 for various values of the parameter λ. Additional plots of the physical variables are presented in Figs. 4 to 7, with Teflon taken as the subliming material.

Consider now modification of the above analysis to the case of a melting material. In this case, consistent with the assumption of instantaneous removal of the melted material, Eq. (14) is replaced by $q(t)=q_0$ which is mathematically equivalent to setting $\Pi=0$ in Eq. (14) and in the definition of λ, Eq. (20). The remaining formulation is identical. Evidently T_s and L are now interpreted as the melting temperature and heat of fusion, respectively. The corresponding time required for the surface to reach the melting temperature will be denoted by t_m.

It is of interest to compare the results for the melting material with the analysis of Landau (reference 7). With the exception of the boundary condition which is assumed to apply before melting starts, both analyses treat an identical problem.[*] Comparison of the two theories indicates that the expressions derived for the steady state ablation velocity [Eq. (29)] and the steady state temperature profile [Eq. (28)] are identical with the results of reference 7. The amount of material which is removed, as predicted by the two theories, is shown in Fig. 8 in terms of the nondimensional variables of reference 7. We note that the agreement is good for physical times corresponding to test conditions. The large deviation which occurs at very

---

[*] In reference 7 it is assumed that for all $t \geq 0$, $q(t)$ is constant at the surface, while in the analysis here the boundary condition at the surface is taken as $h=q(t)/[T_\infty-T(0,t)]=$constant. Evidently for $t \geq t_m$ these conditions are equivalent, since it is assumed that the surface remains at this temperature thereafter. The two problems will therefore differ solely in the manner in which t_m is evaluated. For the conditions under which the experimental portion of this report was performed this difference has a negligible effect on numerical results.
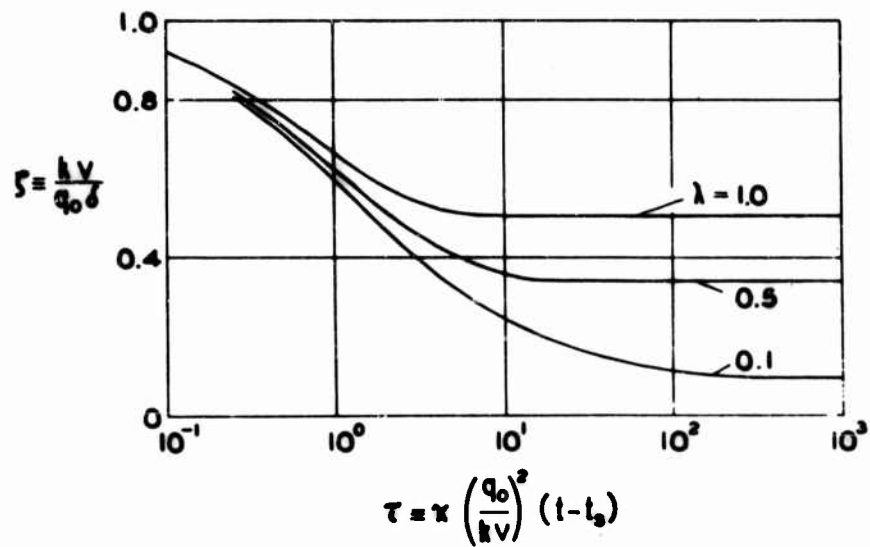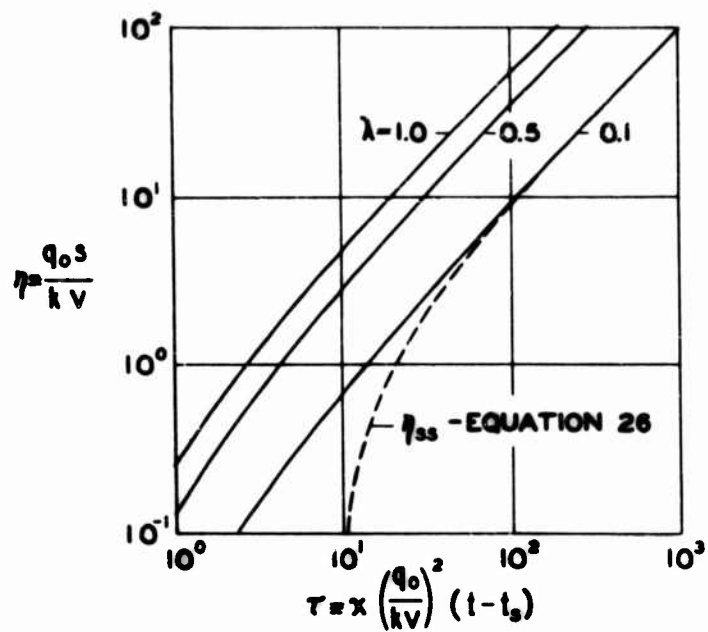
FIG. 3 LOCATION OF VAPORIZATION LINE AND THERMAL
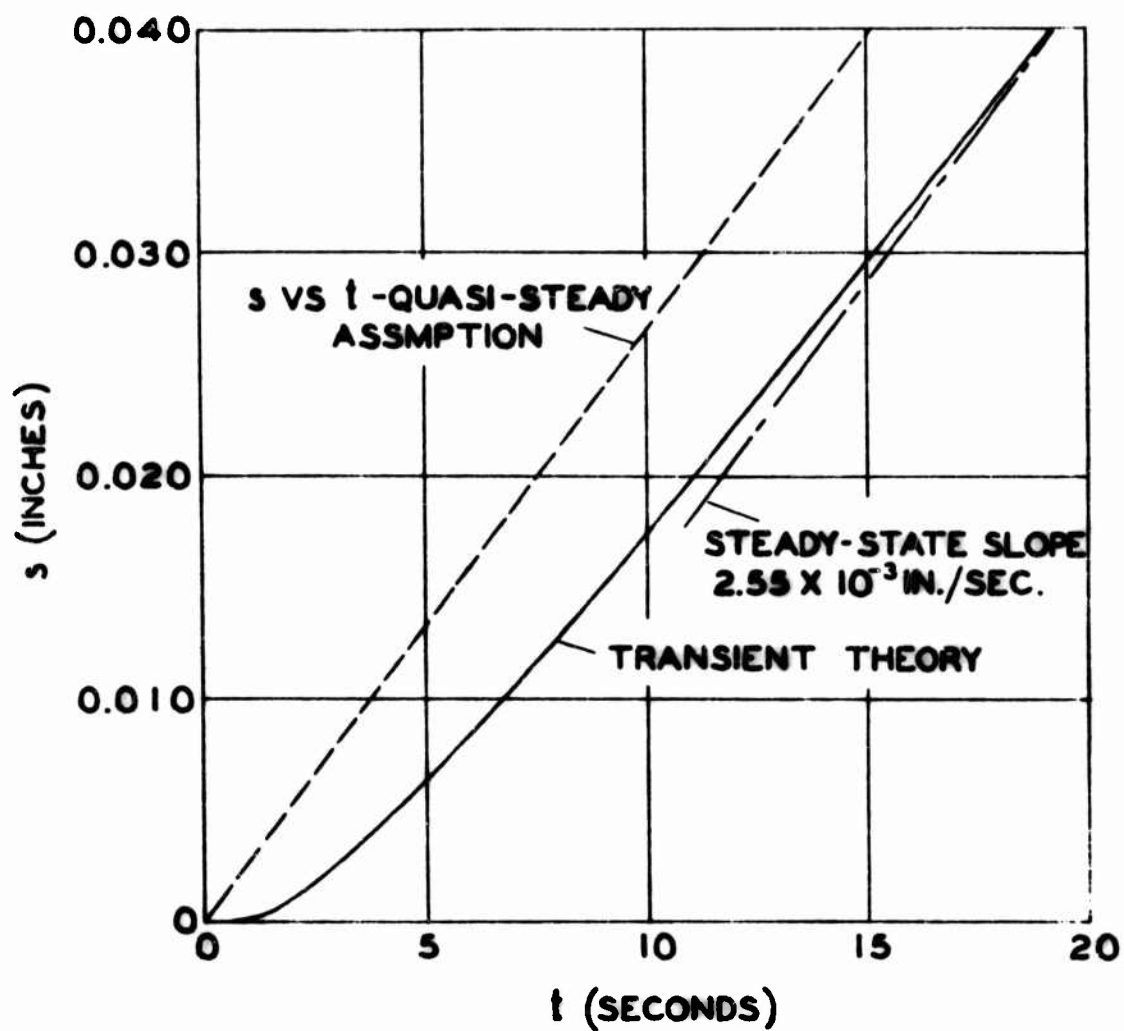PENETRATION (NON-DIMENSIONAL)

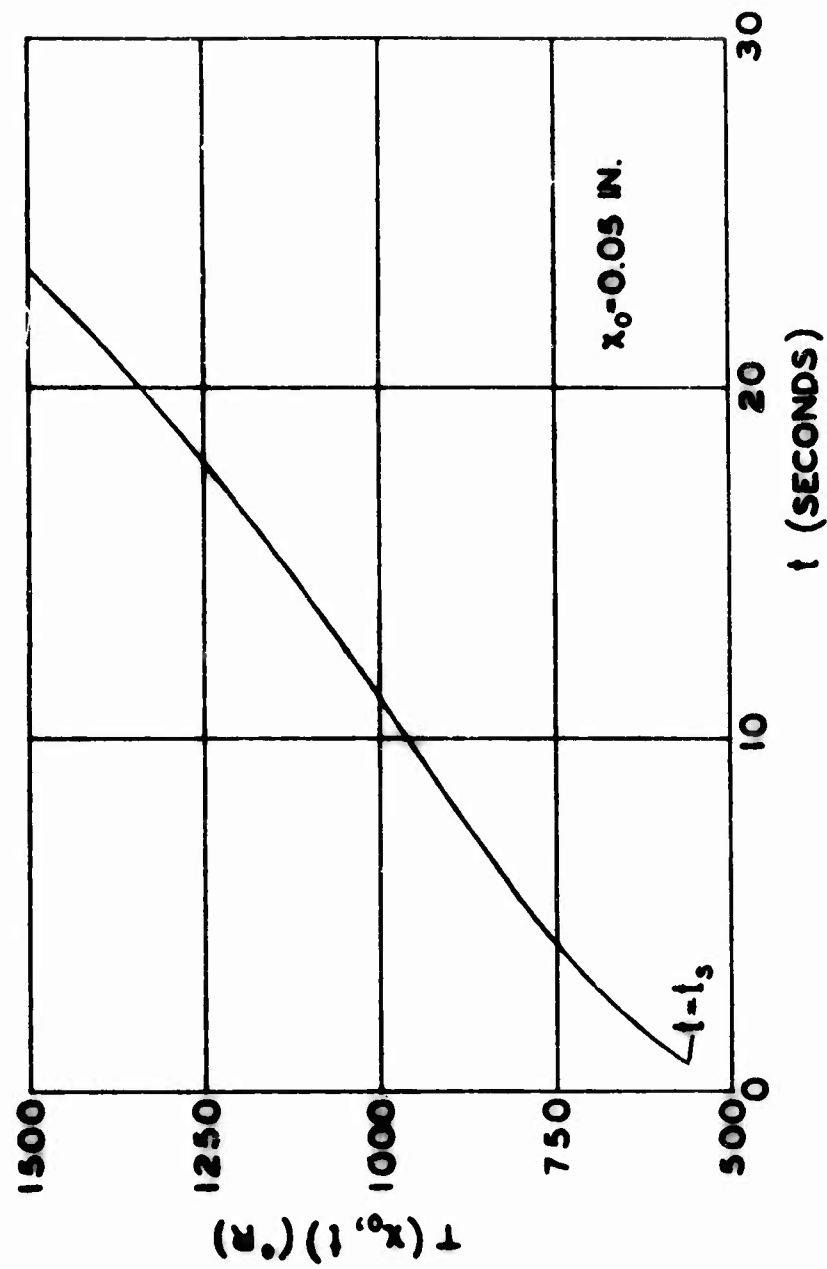FIG. 4 LOCATION OF VAPORIZATION LINE VS TIME
MODEL T-10. $\bar{s} = 0$

FIG. 5 TEMPERATURE HISTORY AT SPECIFIC DEPTH FOR
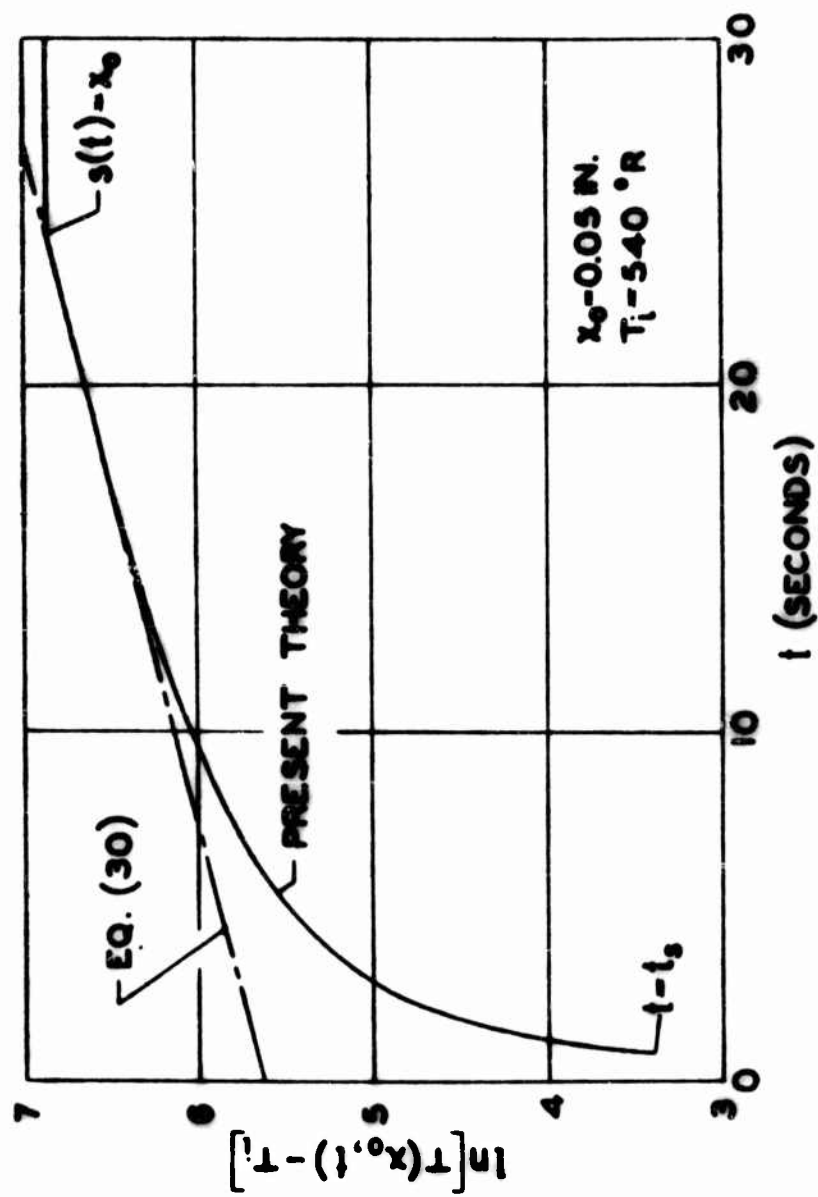MODEL T10 – TRANSIENT THEORY

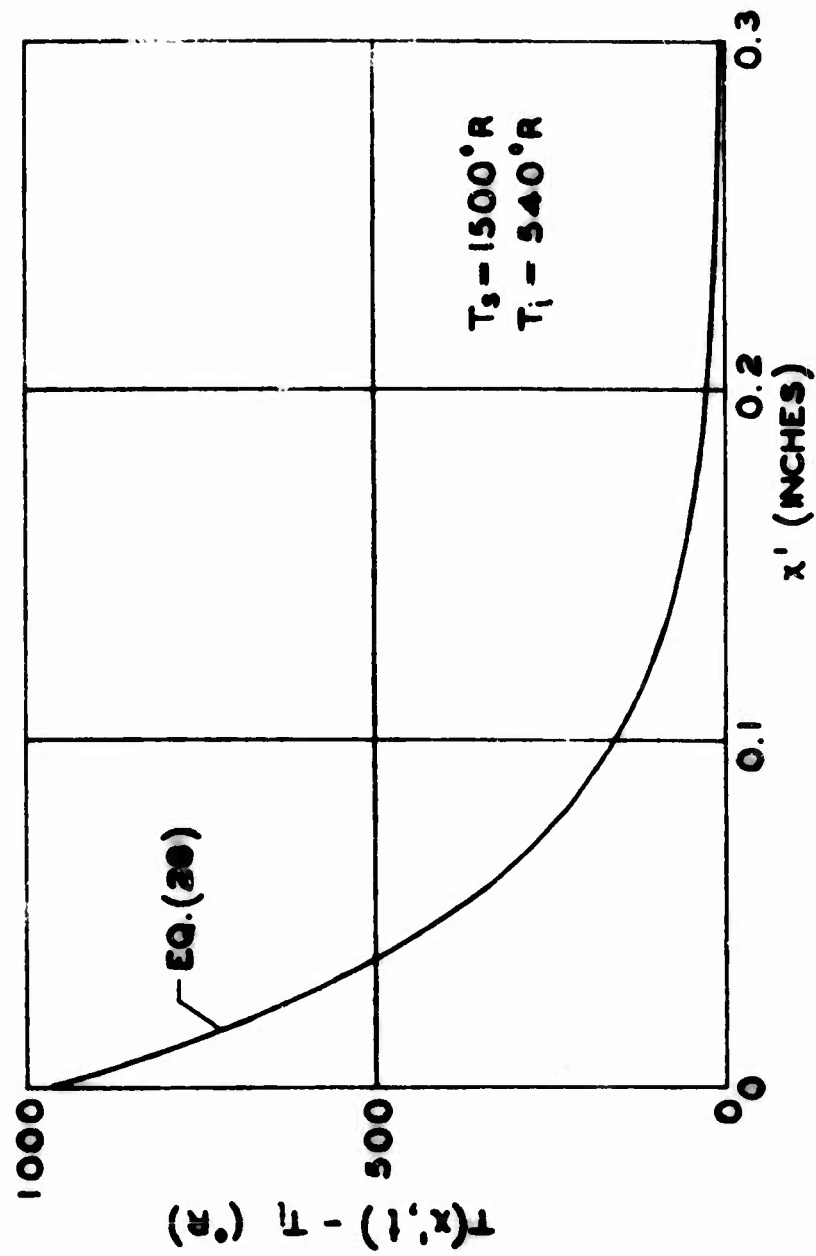FIG. 6 LOG PLOT OF TEMPERATURE HISTORY - MODEL T 10 $\bar{s}-0$

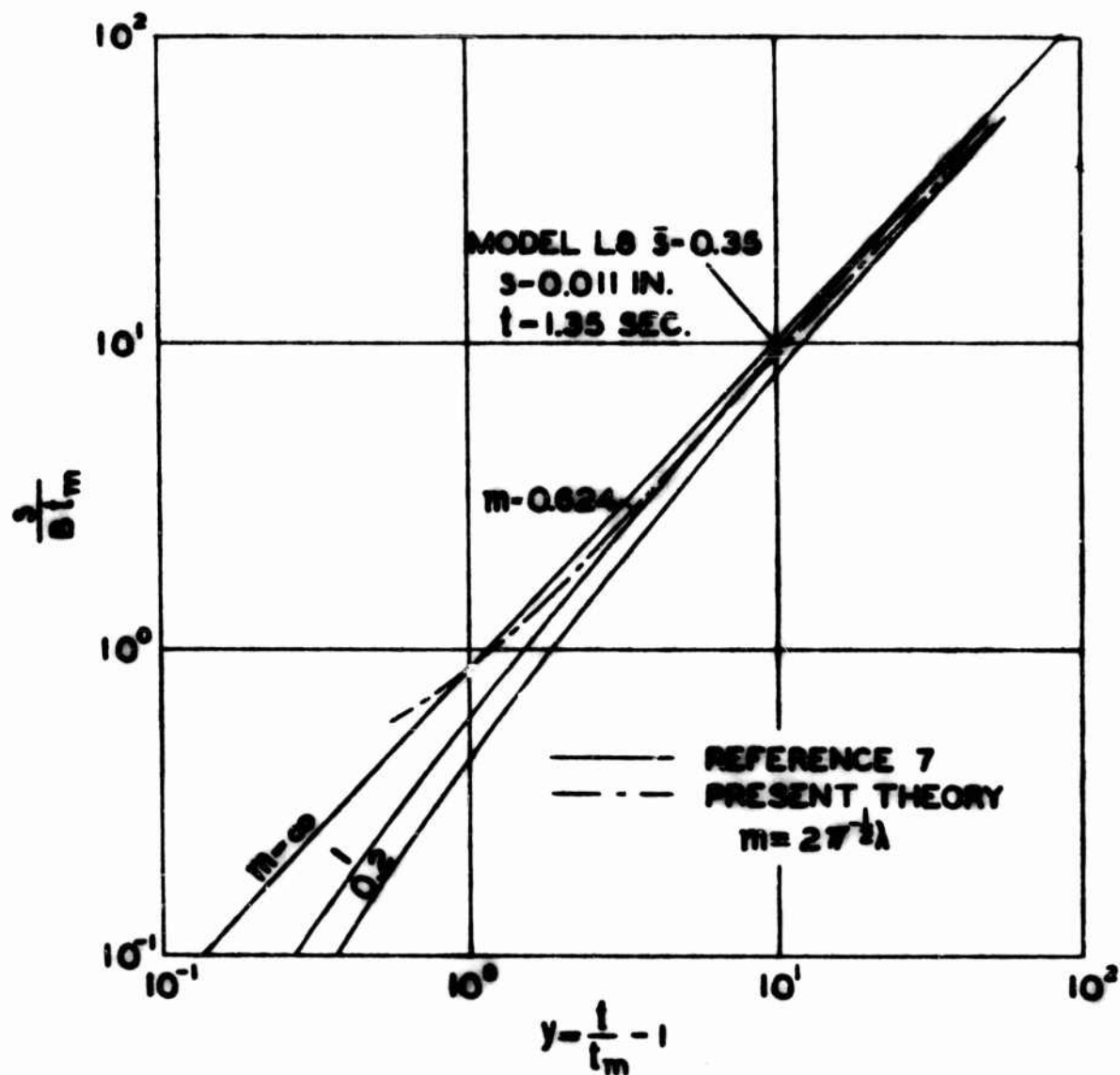FIG. 7 STEADY STATE TEMPERATURE DISTRIBUTION
FOR MODEL T10

FIG. 8 COMPARISON OF PRESENT THEORY WITH
RESULTS OF REFERENCE 7

short times is due to the previously mentioned difference in the values of t_m.

As has been previously noted in the introduction, the assumption of instantaneous removal of the melted material effectively neglects the interaction between this liquid and the external flow. More detailed analysis reveals that this interaction tends to reduce the interface heat flux resulting in a decrease in the rate at which material is removed (cf. reference 10). Thus the more elementary theory considered here will predict higher values for the ablation rates, and in this sense it is conservative. This point will be considered again in connection with the experimental results which were obtained.

Finally, it is interesting to note that one may deduce the thermal diffusivity $\varkappa$ of the plastic materials experimentally by utilizing the analysis presented above. The technique is due to Sutton (reference 35) and will be described below.

Consider the expression which has been deduced for the steady temperature distribution, Eq. (28):

$$T(x,t) - T_i = (T_s - T_i) \exp(-\frac{B}{\varkappa} x')$$

where B is the steady-state ablation velocity. Here x' is the distance from the subliming surface and is given in the steady condition by

$$x' = x - Bt + C$$

If we consider the temperature history at a point initially x_0 distant from the surface we have for the temperature history at this location

$$T(t) - T_i = (T_s - T_i) \exp[-\frac{B}{\varkappa}(x_0 - Bt + C)]$$

Taking the logarithm of this equality, we obtain

$$\ln[T(t) - T_i] = D + \frac{B^2 t}{\varkappa} \tag{30}$$

where

$$D = \ln V - \frac{B}{\varkappa} (x_0 + C)$$

Eq. (30) will plot as a straight line with slope equal to $\frac{B^2}{\varkappa}$ (see Fig. 6). Hence the semi-log plot of the measured temperature history combined with measurements of the steady-state ablation velocity, yields the experimentally the thermal diffusivity of materials.

B. Steady Ablation

The analyses to be presented here is due to S. Georgiev, et al (reference 14) and is included in order to emphasize some additional parameters which are pertinent to the study of ablation from an engineering point of view.

It has been shown in the previous analysis that when a steady state condition of ablation has been achieved the temperature profiles within the solid remain invariant with respect to the receding surface. In this case the energy within the solid remains constant. During this period, therefore, the heat conduction term may be eliminated from the heat balance at the ablating surface [Eq. (9)] with the result

$$q - q_r = m(c_p V + L) \tag{31}$$

Here m is the steady-state mass loss rate $(m = \rho B)$, a constant, and the remaining symbols retain their previous meaning. Eq. (31) states that the aerodynamic heat transfer to the solid is absorbed by the heat capacity plus the heat of sublimation of the ablating material. It will be noted that an additional term q_r has been included to account for heat radiation from the surface.

The dependence of the aerodynamic heat transfer rate on the injection rate introduced previously [see Eqs. (14) and (A-3)] is again valid and yields, together with Eq. (31):

$$q_o = m\left[\frac{c_p V + L + \frac{2}{3} M^{\frac{1}{6}}(h_\infty - h_s)}{1 - q_r/q_o}\right] \tag{32}$$

If now an effective heat of ablation is defined by $h_{eff} = q_o/m$,

$$h_{eff} = [\frac{c_p V + L + \frac{2}{3} M^{\frac{1}{4}} (h_\infty - h_s)}{1 - q_r/q_o}] \tag{33}$$

Eq. (33) can be modified to account roughly for the effect of any chemical reaction of the injected vapor with the external flow. In reference 36, with the assumptions Lewis number equal to unity, and total reaction of all the oxygen diffusing to the surface, an expression for the increase in interface heat transfer is deduced:

$$\Delta q = \frac{0.21 h_c}{h_\infty - h_s} \, q \tag{34}$$

Here h_c is the heat released per unit mass of oxygen entering into the reaction, and the numerical factor is the mass fraction of O_2 external to the boundary layer. Substitution of Eq. (34) in Eq. (33) yields

$$h_{eff} = [\frac{c_p V + L}{1 + q_c} + \frac{2}{3} M^{\frac{1}{4}} (h_\infty - h_s)] [1 - \frac{q_r}{q_o(1 + q_c)}]^{-1} \tag{35}$$

where

$$q_c \equiv \frac{0.21 h_c}{h_\infty - h_s}$$

It is noted that Eq. (35) predicts no dependence of the effective enthalpy on the heat flux rate in the absence of radiation. In addition, for sufficiently high values of the boundary layer enthalpy difference, the contribution of combustion is also negligible, as has been indicated previously (cf. reference 27).

If the effect of radiation and chemical reaction are neglected, there results a simple linear relation between h_{eff} and the "driving enthalpy" $h_\infty - h_s$:

$$h_{eff} = c_p V + L + \frac{2}{3} M^{\frac{1}{4}} (h_\infty - h_s) \tag{36}$$

For a given material, c_p, V, L, and M are known quantities so that a simple calculation immediately yields the heat absorbing capability of a given material under specified flow conditions. Conversely, a rather simple experimental procedure (i.e., measurement of q_0 and m for various values of $h_\infty - h_s$) permits the determination of the intercept ($c_p V + L$) and the slope ($2/3 M^{1/4}$) of Eq. (36), and thus yields important information concerning the properties of the material.

The results described above have been verified experimentally.

C. Aerodynamic Heating

Under the conditions to which the ablating models were exposed in this investigation both laminar and transitional heating may be expected. Hence, for purposes of comparison a theoretical analysis for both types of heat transfer is required.

The laminar theory utilized is due to Lees (reference 3) with modification for the more accurate stagnation point theory of Fay, Riddell, and Kemp (reference 37). In terms of the nondimensional parameters defined in the List of Symbols this analysis gives

$$\frac{N_{Nu}}{N_R^{\frac{1}{2}}} = \frac{0.67}{2} \left(\frac{\rho_w \mu_w}{\rho_{t_e} \mu_{t_e}}\right)^{0.1} F(\bar{s}) \tag{37}$$

where

$$F(\bar{s}) = \frac{\bar{\rho} \bar{\mu} \bar{u} \bar{r}}{\left[\int_0^{\bar{s}} \bar{\rho} \bar{\mu} \bar{u} \bar{r}^2 d\bar{s}\right]^{\frac{1}{2}}} \tag{38}$$

and the Prandtl number is taken to be 0.71. If an isentropic relation between velocity and pressure is assumed, then, for a given pressure distribution and body geometry $F(\bar{s})$ may be evaluated, using an average isentropic exponent together with isentropic flow tables, such as those

given in reference 38. For specified external flow conditions the heat transfer rate q_o may be computed from the definition

$$N_{Nu} = q_o c_{p_{t_e}} R_o / k_{t_e} (h_{t_e} - h_w) \qquad (39)$$

For comparison with the experimental heat transfer data which were obtained, q_o is evaluated from Eq. (39) for the wall temperature equal to the initial surface temperature of the model; that is, $q_o|_{T_w=T_i}$. On the other hand, the quantity which is required for the calculation of the pertinent ablation parameters is the value of the aerodynamic heat transfer when the wall temperature is equal to the ablation temperature, namely $q_o|_{T_w=T_s}$. This latter quantity is obtained by recalling that the heat transfer coefficient h is constant in the test section; then

$$q_o|_{T_w=T_s} = h(T_\infty - T_s) = [\frac{q_o|_{T_w=T_i}}{T_\infty - T_i}] (T_\infty - T_s) \qquad (40)$$

It should be noted that the value of h varies locally from point to point on the body surface but is a constant at any given station $\bar{s}$.

For the calculation of transitional heat transfer a numerical integration of the momentum equation for the axisymmetric boundary layer was required. This equation may be written in the form

$$\frac{dN_{R_\vartheta}}{d\bar{s}} = N_R \frac{\bar{\rho} \bar{u}}{\bar{\mu}} \frac{c_f}{2} - N_{R_\vartheta} \frac{d}{d\bar{s}} (\ln \bar{r} \bar{\mu}) \qquad (41)$$

where

$$N_{R_\vartheta} = \rho_e u_e \vartheta / \mu_e,$$

$$\vartheta = \int_0^\infty (\rho u/\rho_e u_e)(1-u/u_e)dn \quad \text{the momentum thickness,}$$

n = coordinate normal to the wall, and

$c_f = 2 \tau_w / \rho_e u_e^2$, the local skin friction coefficient.

For the integration of Eq. (41) the relation between the skin friction coefficient and N_{R_ϑ} must be known. In accordance with the suggestion of Persh (reference 39) and including the modification of reference 40, the skin friction law used here was

$$\frac{c_f}{2} = \bar{\mu}[0.013 \, N_{R_\vartheta}^{-\frac{1}{4}} - K N_{R_\vartheta}^{-a}] \tag{42}$$

where K is selected such that $c_f/2$ is continuous at transition. In reference 39, on the basis of experimental data from flat plate transition, it is concluded that a=2. The results here suggest that in a favorable pressure gradient the transition zone may be more extended; accordingly, a value of a=1 was assumed. The initial value of N_{R_ϑ} at the start of transition is obtained from the relation

$$\frac{N_{R_\vartheta}}{N_R^{\frac{1}{2}}} = \frac{0.66[\int_0^{\bar{s}} \bar{\rho}\,\bar{\mu}\,\bar{u}\,\bar{r}^2 d\bar{s}]^{\frac{1}{2}}}{\bar{r}\,\bar{\mu}} . \tag{43}$$

This expression corresponds to the laminar theory of Lees cited previously. Eq. (41) may now be integrated from the transition point (determined experimentally) and yields the skin friction and momentum thickness distributions. For the calculation of the corresponding heat transfer distribution, Reynolds analogy (valid for the "cold wall" case; cf. reference 40), modified to account empirically for nonunity Prandtl number effects, is used. There results

$$q_o = \sigma^{-\frac{2}{3}} (h_{aw} - h_w) \rho_e u_e (c_f/2) \tag{44}$$

where $\sigma \equiv$ Prandtl number and h_{aw} is the adiabatic wall enthalpy defined by the equation

$$\frac{h_{aw} - h_e}{h_{t_e} - h_e} = \sigma^{\frac{1}{3}} \tag{45}$$

In terms of the Nusselt number N_{Nu}, Eq. (44) may be written

$$N_{Nu} = 0.89(c_f/2) GN_R \overline{\rho}\ \overline{u} \tag{46}$$

where $G \equiv (h_{aw} - h_w)/(h_s - h_w)$ and the Prandtl number is again taken as 0.71. Integration of Eq. (41) was carried out numerically on the PIBAL Bendix G-15 General Purpose digital computer by the Runge-Kutta method.

For fully developed turbulent heat transfer the prediction of the flat plate reference enthalpy method (cf. Method I of reference 41) has been used.

D. General Remarks

It is evident from the foregoing that the fundamental measurements to be obtained for the study of steady subliming ablation are the quantities q_o and m. For the transient case a time resolved history of the surface recession s(t) would be required. It would also be of interest to obtain the temperature-time history $T(x_o, t)$ at some point below the surface of the ablating material for comparison with the transient theory which has been developed. These quantities should, of course, be measured over a range of stagnation conditions, so that their variation with $h_\infty - h_s$ and q_o may be established. Certain additional information such as stagnation temperature and pressure as well as the existing pressure distribution is also required.

In the following sections the facility recently developed at the PIBAL, expressly for the study of ablation, is described. A description

of the models and test procedure used to obtain experimentally the neces-
sary information is also included.

III. DESIGN AND DEVELOPMENT OF THE FACILITY

The facility which has been constructed for the experimental inves-
tigation of ablation is depicted schematically in Figs. 9, 10, and 11. It is
a supersonic, blowdown wind tunnel with an axisymmetric, open jet test
section approximately six inches in diameter. This tunnel is connected to
the multiple outlet of the hypersonic test facility described in references 42
and 43. A pebble-bed heater with a design temperature of $3000^{\circ}R$ and a
maximum pressure of 600 psia is the basic energy source used in connection
with several tunnels and special test rigs.

The nozzle is a fixed geometry, axisymmetric, contoured nozzle,
which provides flow at Mach number 4.4. Although fabricated entirely from
type 304 stainless steel, the subsonic and throat regions of this nozzle are
cooled by a mixture of air and water at stagnation pressures varying from
150 to 600 psia, depending on the nozzle stagnation conditions.

The contours for the supersonic portion of the nozzle were taken
from reference 44. Corrections for boundary layer growth were made
according to the method developed by Ruptash (reference 45) to compute the
displacement thickness. The nozzle Mach number was chosen to be 4.4 in
order that the tunnel could be exhausted directly to the atmosphere. Although
the PIBAL facility has available a vacuum system capable of reducing back
pressure to less than 1/2 psia, it was decided not to exhaust to this system
during ablation tests because of the possible generation of corrosive products.
Hence, since the stagnation pressure has an upper limit (i.e., 600 psia), the
Mach number chosen was that believed to be the maximum for which the
tunnel could be started with a crude diffuser and/or ejector.

The arrangement of the test section is shown schematically in
Fig. 10. An open jet configuration was utilized so that the ablating models
could be introduced into and retracted from the air flow at well defined
times. The time interval required for the model to reach its fully inserted
position is on the order of 1/10 second. A pneumatic cylinder activated
the model support system.
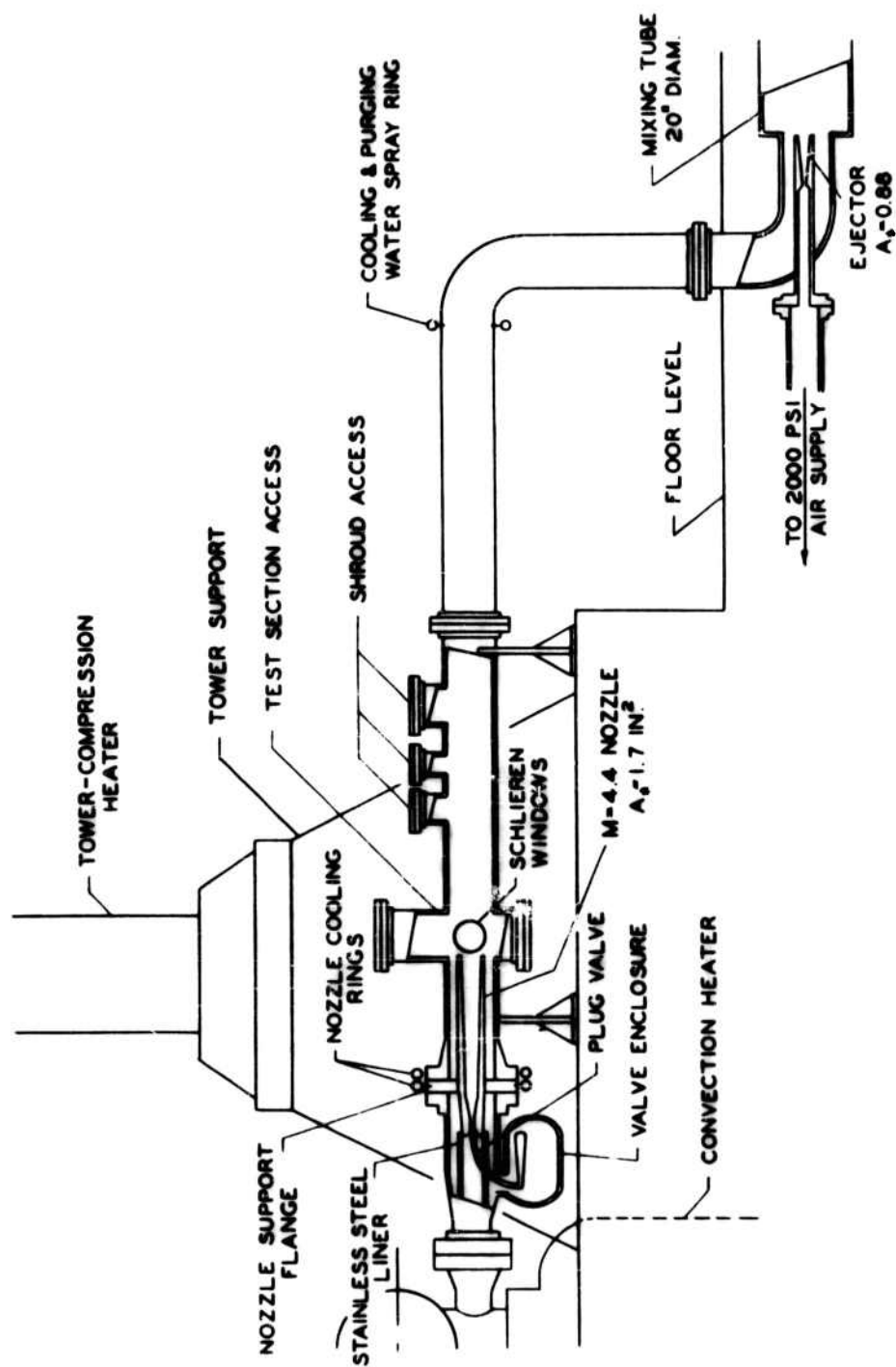
FIG. 9 GENERAL SCHEMATIC – MACH 4.4 WIND TUNNEL

Labels in figure:

TOWER-COMPRESSION HEATER

TOWER SUPPORT

TEST SECTION ACCESS

SHROUD ACCESS

COOLING & PURGING WATER SPRAY RING

MIXING TUBE 20" DIAM.

NOZZLE COOLING RINGS

SCHLIEREN WINDOWS

M–4.4 NOZZLE $A_t \approx 1.7$ IN^2

NOZZLE SUPPORT FLANGE

STAINLESS STEEL LINER

PLUG VALVE

VALVE ENCLOSURE

CONVECTION HEATER

FLOOR LEVEL

TO 2000 PSI AIR SUPPLY

EJECTOR $A_t \approx 0.88$
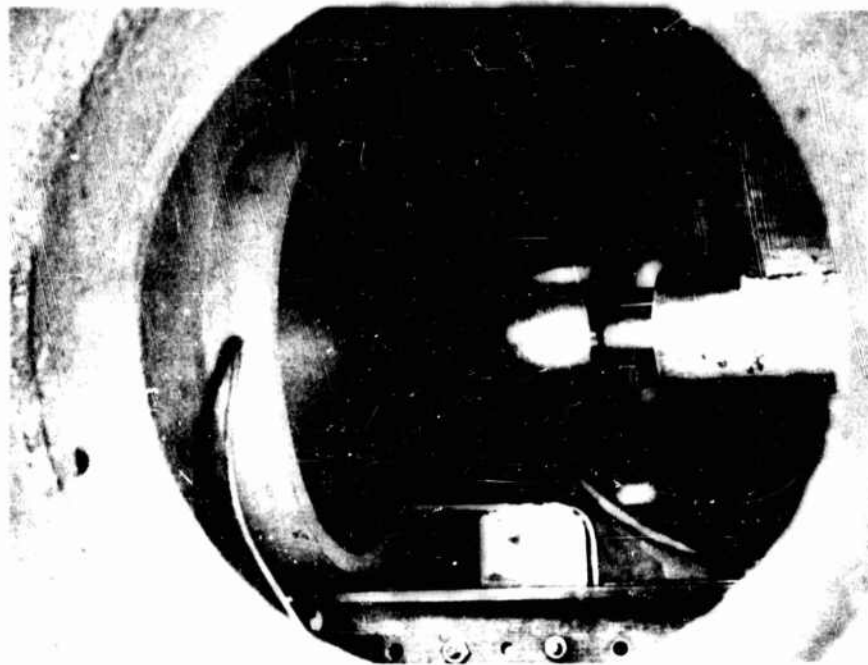
TEST SECTION - CALORIMETER IN POSITION
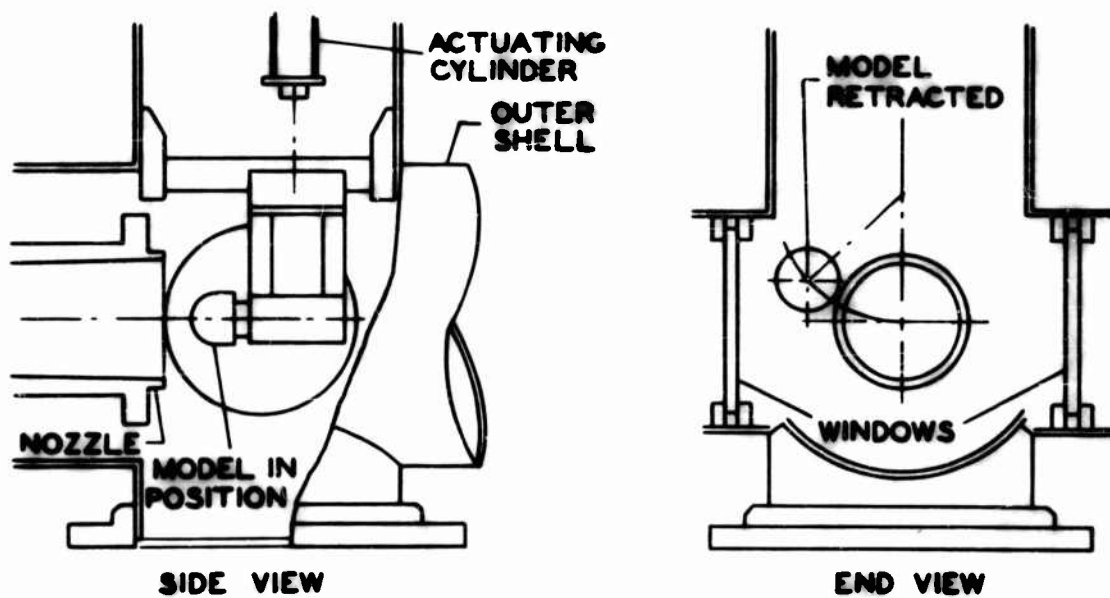
SCHEMATIC OF TEST SECTION

FIG. 10. DETAILS OF TEST SECTION INSTALLATION
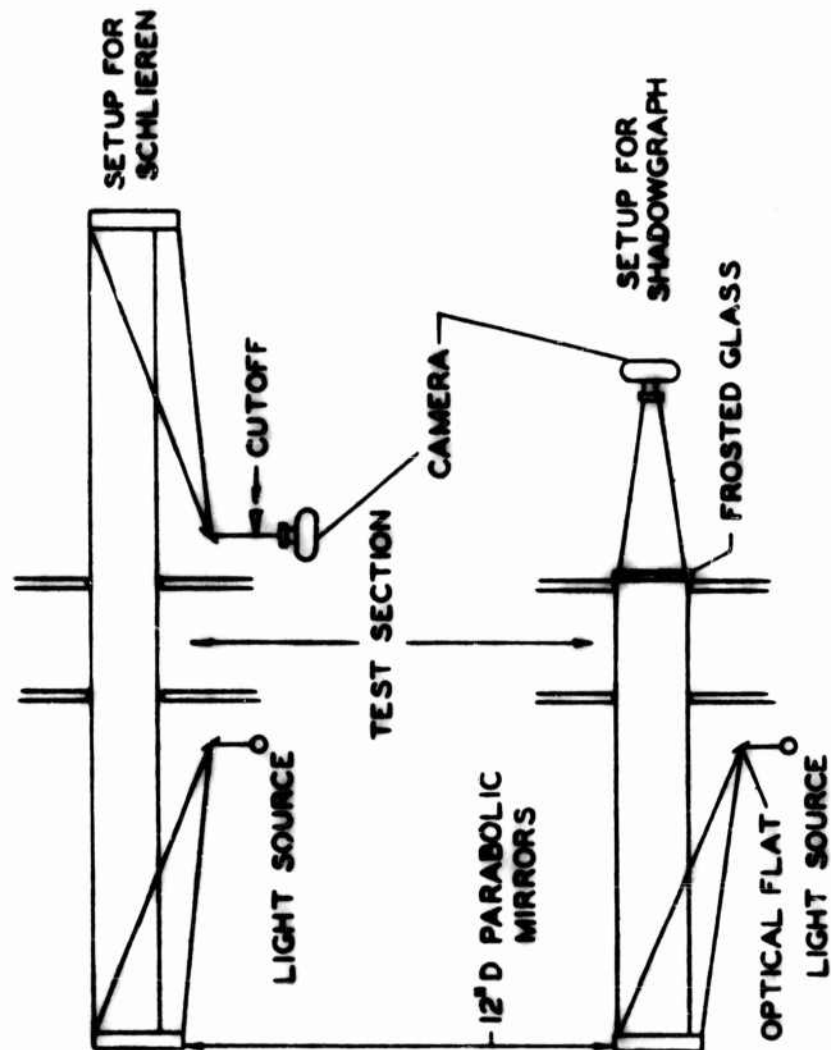
FIG. 11 SCHEMATIC OF OPTICAL SYSTEM

The optical system shown in Fig. 11 utilizes two 12-inch diameter parabolic mirrors with 4-foot focal length for schlieren photographs, while for shadowgraph pictures only one is used as shown in Fig. 11. The test section is provided with 10-inch diameter windows of one-inch thick, good (but not optical) quality plate glass set in steel frames. These are tilted at an angle of 5° to the axis of the mirrors to eliminate extraneous reflections. It is to be noted that frosted glass is added to the window nearest the camera when the shadowgraph technique is used. The knife edge, light source and cameras are installed outside the protective enclosure. Adjustment and alignment of the optical system can be accomplished externally.

It was originally assumed that sufficient diffusion could be provided by an axisymmetric diffuser and considerable effort was expended to make a suitable diffuser. Starting was achieved for an empty test section configuration with an area ratio (diffuser throat to test section area) of 1.26. However, tunnel start with a three-inch diameter blunt model was not achieved. It was found necessary to use ejectors to reduce back pressure.

The ejector and mixing tube are shown schematically in Fig. 9. With a throat area of 0.88 in. and with supply conditions $T_{stag}=540^\circ R$, $P_{stag}=2000$ psia, approximately $34\#/sec$. of mass flow is provided. Tests have indicated that the test section pressure is reduced by about 50 percent by this ejector, and starting with the aforementioned model has been successfully achieved for heater pressures greater than 500 psia. Detailed discussion of this type of starting technique may be found in reference 46.

An additional feature of the exhaust system is the water spray for cooling and purging of the heater air prior to exhaust to the atmosphere. The ejector air also provides additional cooling.

IV. DESCRIPTION OF MODELS,
TEST PROCEDURE AND INSTRUMENTATION

A. Description of Models

The parameters which are of interest in ablation tests have been described in Section II. For the experimental determination of these quantities two types of models have been designed and fabricated. The first of

these, which will be referred to as the calorimeter, is shown in Figs. 12 and 14... This model is used to determine experimentally the zero ablation heat transfer rates (q_0) and the pressure distribution. The calorimeter was fabricated from number type 304 stainless steel with a wall thickness of 0.050 inches; it was instrumented with surface pressure taps and iron-constantan thermocouples located as shown in Fig. 12. To insure that the thermocouples read the surface temperature of the calorimeter, the installation was accomplished in the following manner: A 0.040 inch diameter hole was drilled through and perpendicular to the surface of the model; the thermocouple wire was passed through the hole and held in place by driving a stainless steel tapered pin into the hole from the outside, crushing the wires together at the outer surface of the model. The pin was then filed flush with the model surface. The external geometry of the calorimeter is, of course, identical with the plastic ablators which are described below. The thickness chosen is consistent with the transient technique which is utilized to determine the surface heat transfer rates.

The geometry chosen for the ablating specimens was based on the following requirements: that the models

(a) be large enough to permit measurements to be obtained around an extended surface and to provide transitional and turbulent flow;

(b) have a configuration which would be of practical interest and at the same time be of the simplified type for which detailed analysis is available;

(c) be sufficiently thick for a semi-infinite slab analysis to apply, and for the installation of temperature sensing devices below the surface.

The final configuration chosen is shown in Figs. 13 and 14 ; also shown are the location and depth of the thermocouples which are imbedded in the plastic. It will also be noted that a stainless steel, cylindrical, afterbody has been added to the model mount. This skirt has been instrumented with surface thermocouples identical to those on the calorimeter. It should be noted that the values of q_0 thus obtained correspond to the zero ablation case since they are evaluated with the surface temperature equal to the initial temperature at which time no ablation of the plastic models has occurred.

The installation of the thermocouples on the plastic models was accomplished as follows: a series of 0.125-inch diameter holes were drilled

FIG. 12 DETAILS OF CALORIMETER AND INSTRUMENTATION
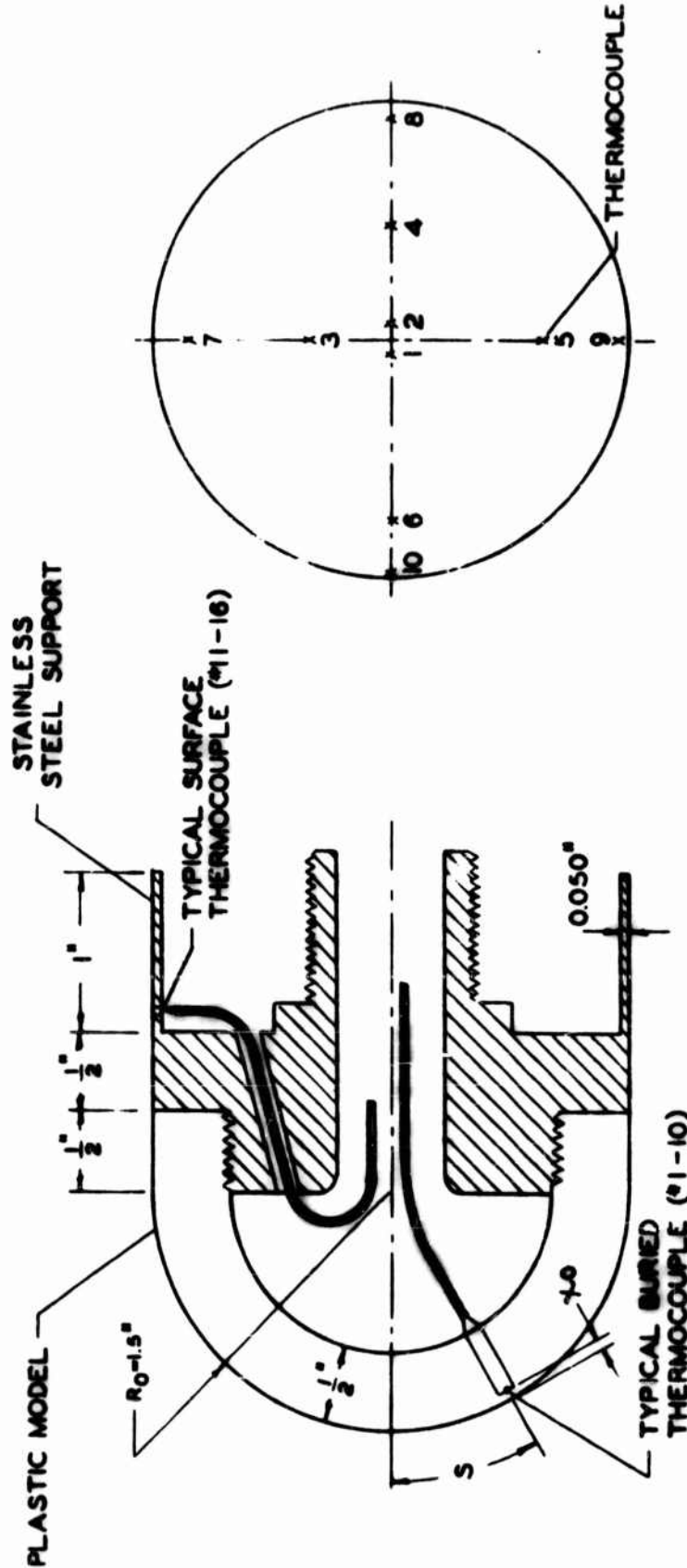
THERMOCOUPLE #	1	2	3	4	5	6	7	8	9	10	11,11A	12,12A	13,13A	14,14A	15,15A	16,16A
s−S/R₀	0.013	0.349	0.524	0.698	0.873	1.047	1.222	1.398	1.484	2.023	2.119	2.214	2.309	2.405	2.500	—
x₀	0.060	0.050	0.050	0.050	0.050	0.050	0.050	0.050	0.050	—	—	—	—	—	—

FIG. 13   DETAILS OF ABLATING MODELS AND INSTRUMENTATION
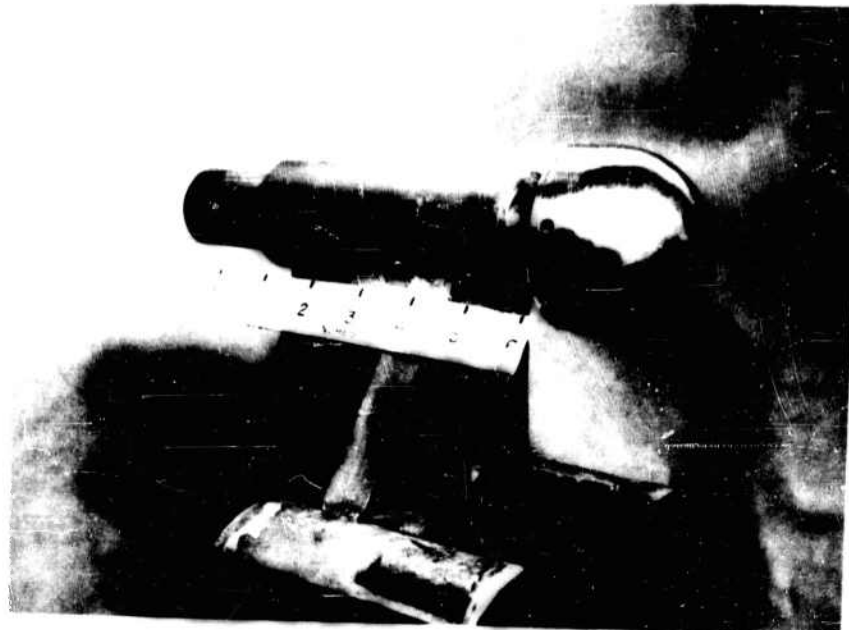
CALORIMETER

ABLATING MODEL

FIG. 14. TYPICAL MODEL CONFIGURATIONS

through the plastic models in the radial direction. Plugs of approximately 0.125-inch diameter of material identical to that of the model were then fitted with iron-constantan thermocouples at the desired depth as shown in Fig. 15. These plugs were thereupon pushed into the holes in the model from the rear or concave side till the external ends could be machined to match the hemispherical surface of the models. Due to the natural flexibility of the plastic materials the installation was essentially a "force fit" (i.e., the diameter of both the plug and the hole was essentially the same) and, as a result, a very smooth model surface was obtained (see Fig. 14).

Thirteen plastic models were fabricated, identical in size and shape and differing only in the material which was used. A list of these is provided in Table I along with data concerning the type of material, numbering, etc.

Some comments concerning requirement (a) above would be appropriate here. Several investigators have found (see references 4 and 47) that for values of $N_{R_\theta} > 300$ transition will occur. This criterion was used to select the diameter of the models. Preliminary calculations based on a hemispherical geometry and a Newtonian pressure distribution using Eq. (43) indicated that for a model of 3" diameter a value of N_{R_θ} equal to 300 would occur at a latitude of approximately 60°. Fig. 16 shows the actual variation of N_{R_θ} with $\bar{s}$ as obtained from the experimentally determined pressure distribution on a 3" diameter hemisphere (Fig. 17).

B. Test Procedure and Tunnel Conditions

The experimental procedure is as follows: With all recording potentiometers running and the heater stagnation pressure and temperature at the desired values, hypersonic flow is established by first activating the ejector and then withdrawing the valve in the throat of the nozzle. The plastic model is then rotated into the stream; this motion activates a motion picture camera and an electric clock, so that the model and clock are photographed simultaneously and continuously from the instant of exposure. The model is withdrawn prior to tunnel shutdown, the total time of exposure thereby being recorded. The procedure is identical in the case of the heat transfer runs with the calorimeter model except that motion pictures are not necessarily taken.

Test running times are sufficient to achieve steady state ablation on a major portion of the model. (Note that because of the varying local values of q_0 the steady state ablation rate occurs at varying times on the

TABLE I

LIST OF ABLATING MODELS AND VALUES OF PHYSICAL PROPERTIES USED IN CALCULATIONS

Model No.	T1,T5 T10,T12	L8,L9 L11,L13	P2,P6	N3,N7	P4
Material	Teflon	Lucite	Polyethylene	Nylon	Polypropylene
Monomer (formula)	C_2F_4	$C_5H_8O_2$	C_2H_4	-	C_3H_6
Density ρ(lb./in.^{3})	0.080	0.042	0.033	0.041	0.033
Thermal Conductivity k(Btu/in.sec.$^\circ$R)	0.33×10^{-5}	0.22×10^{-5}	0.3×10^{-5}	0.45×10^{-5}	-
Thermal Diffusivity x(in.^{2}/sec.)	1.4×10^{-4}	1.24×10^{-4}	2.7×10^{-4}	1.83×10^{-4}	-
Sublimation (T_s) or Melting Temp. (T_m) ($^\circ$R)	1500	1200	1160	1060	-
Heat of Sublimation L (Btu/lb. Monomer)	750	450	1090	1500	-

#78 DRILL

0.050'(TYP)

½"

TYPICAL PLUG

MODEL SURFACE

JUNCTION

INSULATION

THERMOCOUPLE INSTALLED

#30 GA. IRON-CONSTANTIN
THERMOCOUPLE WIRE

STEP NO. 1

SPOTWELD JUNCTION

INSULATION

STEP NO. 2

JUNCTION PULLED
INTO PLACE

STEP NO. 3

MODEL SURFACE

⅛" DIAM. HOLE

PLUG INSERTED FROM
REAR OF MODEL
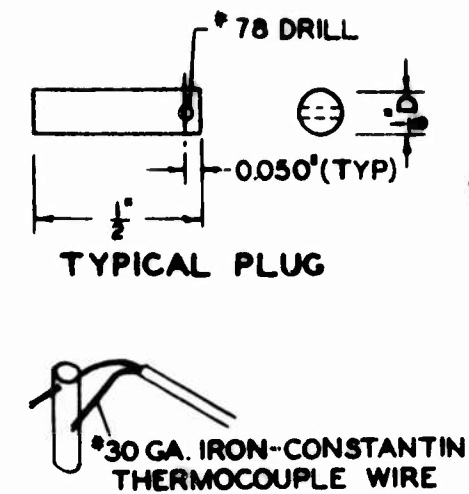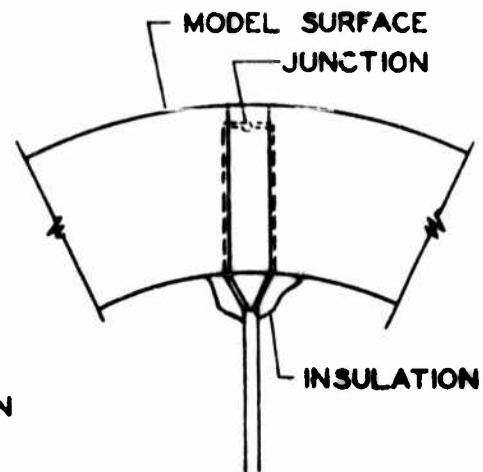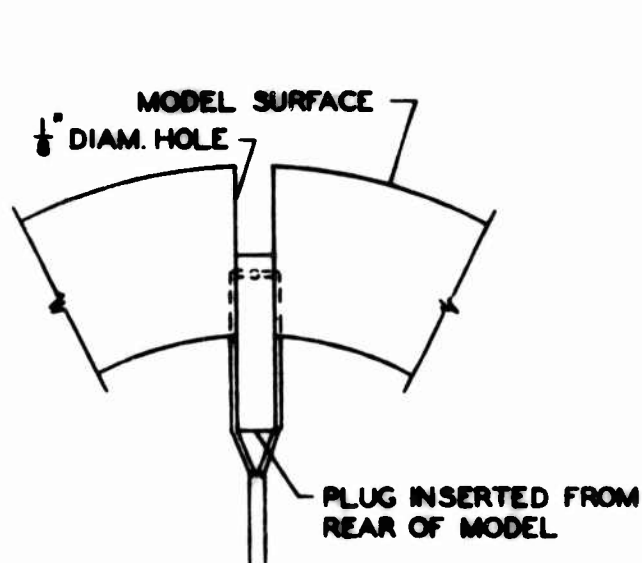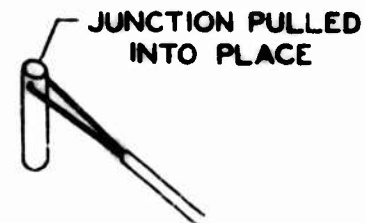
STEP NO. 4

FIG. 15 DETAILS OF THERMOCOUPLE INSTALLATION FOR ABLATING MODELS
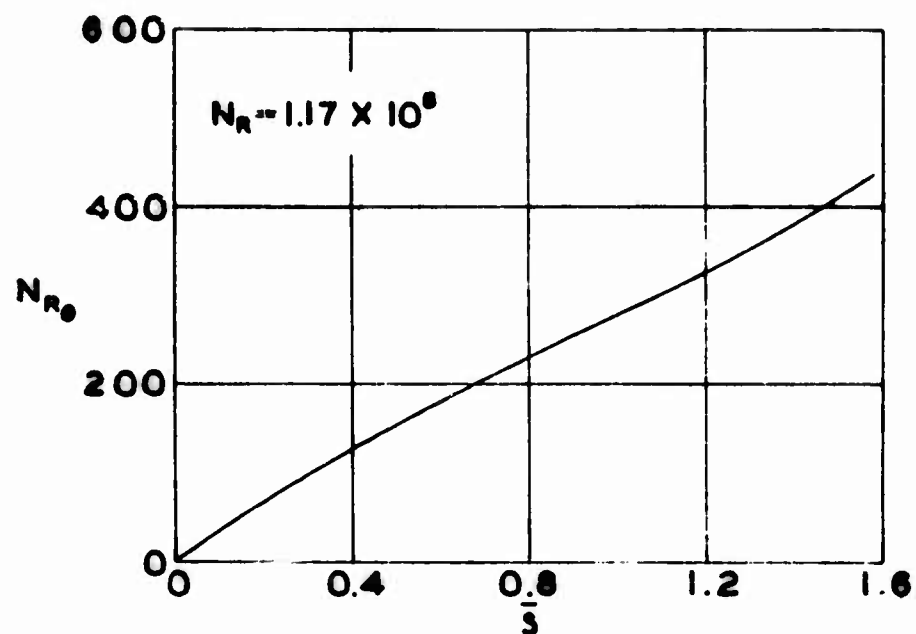
FIG. 16 DISTRIBUTION OF MOMENTUM THICKNESS
REYNOLDS NUMBER FOR PRESSURE DISTRIBUTION
OF FIG. 17
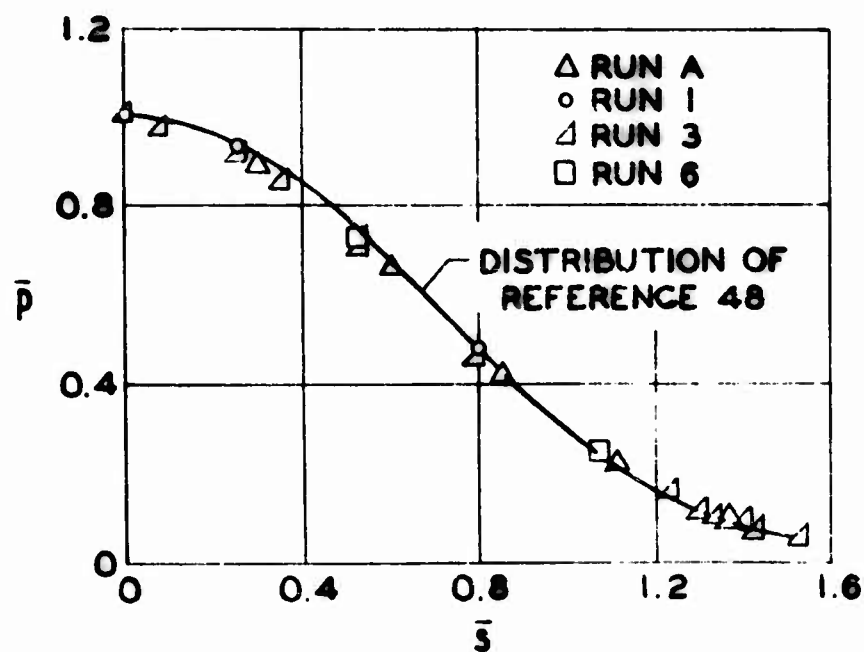
FIG. 17 PRESSURE DISTRIBUTION

model.) These times are estimated to be from 10 to 15 seconds (see, for example, Fig. 4). Table II summarizes the test section conditions to which the models were exposed.

C. Instrumentation

The pressures on the surface of the calorimeter are measured during the test on transducers and recorded on single-channel recording potentiometers. The pitot pressure and stagnation temperatures are measured on probes mounted on brackets attached to the end of the nozzle. A schematic of the temperature probe as well as a photograph are shown in Figs. 18 and 19. All of the model thermocouples are also recorded on recording potentiometers.

Because of the open jet configuration which is used, shielding of all the sensing leads is required. This is complicated by the motion of the model support which is necessary for retraction of the model. The shielding was ultimately accomplished by passing the leads through a stainless steel, pressure tight flexible hose as manufactured by the Titeflex Company. Fig. 20 shows a model mounted on its support to which is also attached the aforementioned flexible hose.

The clock (see Fig. 21), which provides time resolution of the surface recession, was especially built for this purpose. For the drive a synchronous motor with a speed of 2 r.p.m. was utilized in combination with bevel gears with a 2:1 gear ratio yielding a clock speed of 4 r.p.m. A back-lighted, frosted glass dial face was provided, scribed with 120 divisions. Thus, time intervals can be read directly in eighths of a second.

The camera which is used for taking motion pictures during ablation runs is a 16 mm. Bell and Howell "Filmo," type 70-H. It is operated by a variable speed electric motor which will give from 8-64 exposures per second. A camera speed of 64 frames per second has been used with acceptable results. The lens which is used is a Pan-Cinor, wide angle lens f2.8. A Tiffen series 8 - #2 Portra-lens is utilized in conjunction with it, giving a field diameter of 10 inches at a subject-to-lens distance of 24 inches.

The clock and camera are activated from a pressure switch connected to the activating cylinder of the model support, so that the clock and camera start as the model is exposed to the flow.

TABLE II

TEST CONDITIONS ($R_o=1.5$ in., $M_\infty=4.4$)

Run No.	P_t (psia)	T_∞ (°R)	h_∞ Btu/lb.	N_R	λ	t_t (sec.)	s_t (in.)	h_{eff} Btu/lb.
A	60.0	--	--	--	--	--	--	--
1	60.4	--	--	--	--	--	--	--
3	59.0	--	--	--	--	--	--	--
4	61.3	2046	517	1.20×10^6	--	--	--	--
5	56.5	1686	420	1.47×10^6	--	--	--	--
6	61.3	1989	500	1.24×10^6	--	--	--	--
7	61.3	1980	500	1.24×10^6	--	--	--	--
T5	56.5	1925	484	1.19×10^6	0.35	13.36	0.012	2190
T10	53.5	2080	527	1.04×10^6	0.34	27.78	0.062	1250
L8	55.6	1960	494	1.15×10^6	0.42	9.0	0.090	721
L9	58.4	1904	479	1.24×10^6	0.45	15.41	0.122	748
P2	58.0	1750	436	1.36×10^6	0.29	11.1	0.129	705
P6	56.9	1729	430	1.35×10^6	0.29	9.05	0.103	695
N3	57.0	1836	460	1.26×10^6	0.14	9.9	0.104	745
N7	56.5	1729	430	1.34×10^6	0.14	9.9	0.054	959

Stagnation Point Values

SPOTWELDED JUNCTION
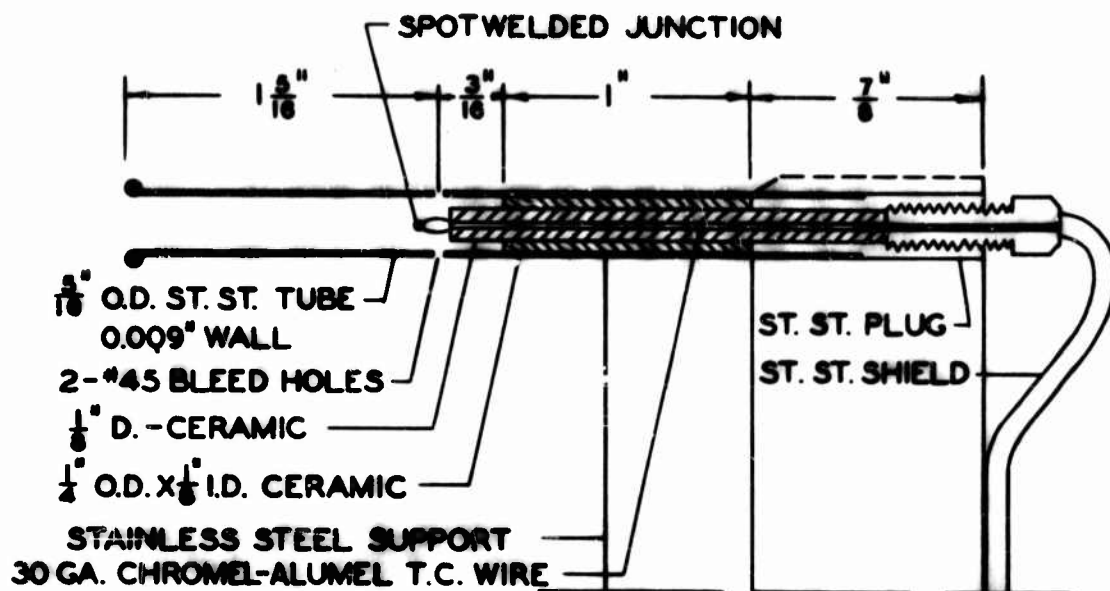
FIG. 18
DETAILS OF STAGNATION TEMPERATURE
PROBE
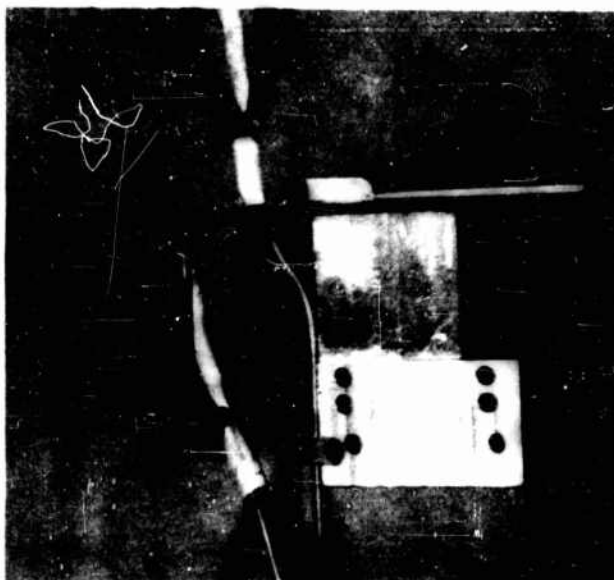
FIG. 19. STAGNATION TEMPERATURE PROBE
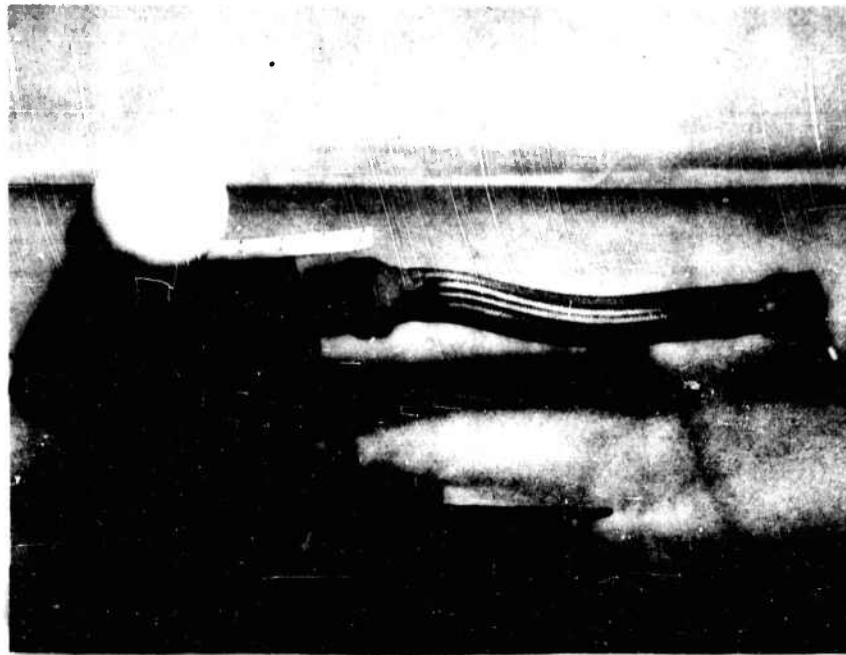
FIG. 20. MODEL AND SUPPORT ASSEMBLY
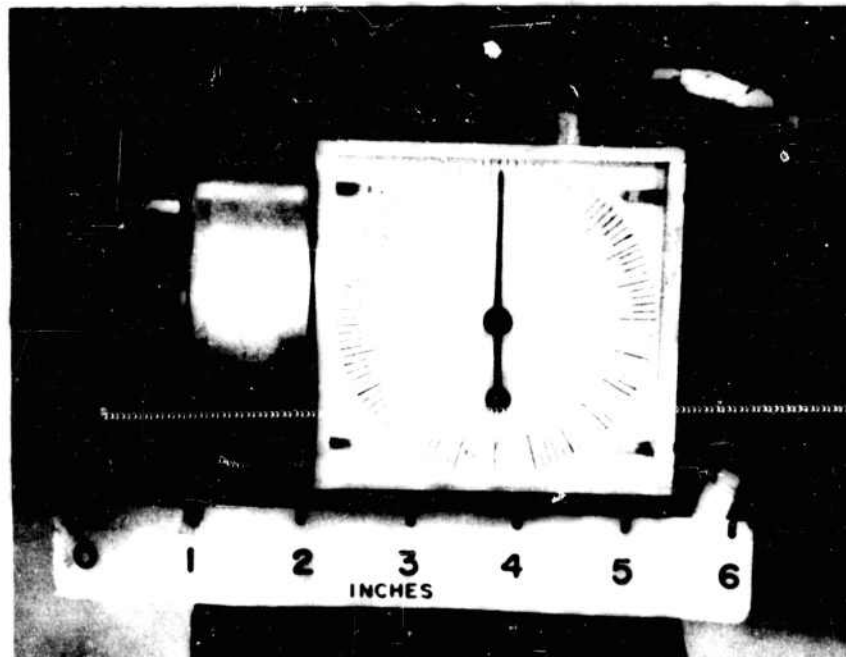
FIG. 21. TIMER

V. DATA REDUCTION

A. Pressure Distribution

The pressure distribution which was obtained from test runs with the calorimeter is presented in nondimensional form in Fig. 17. The results are in good agreement with the modified Newtonian theory of reference 48. Calculation of the theoretical heat transfer distributions which are utilized later are based on these experimental values.

B. Heat Transfer Rates

The local heat transfer rates, q_{o_i}, are obtained from the surface temperature history by the transient technique described in reference 49. Here the subscript i indicates that the calculated values correspond to a surface temperature equal to its initial (i.e., before exposure) constant value, T_i. The data is presented in terms of the Nusselt number N_{Nu} and is plotted against the nondimensional surface coordinate $\bar{s}$ in Figs. 22-25. The results are compared to the laminar and transitional heat transfer theory discussed in Section II, C. of this report. In Fig. 26 there is presented similar data obtained from the cylindrical after bodies during the ablation runs. The calculation for the cylindrical portion is based on the pressure distribution of reference 56 obtained for a body with an identical configuration but at a flow Mach number of 6.

C. Ablation Runs

Of the Thirteen plastic models which were fabricated, eight (two each of four different plastics) were exposed to heated air for times ranging from 9 to 28 seconds. The tunnel conditions and running times for each model are presented in Table II along with other pertinent data.

Although shadowgraph motion pictures were taken of the ablating models, poor resolution of the resulting film did not permit an accurate determination of the time dependent surface recession s(t), and thus also of the steady ablation velocity B or mass ablation rate m (m=ρB). However, the final configuration of the ablators was measured at several azimuthal planes with considerable precision on a Jones and Lamson optical comparator at a magnification of ten. It was found that the models ablated in
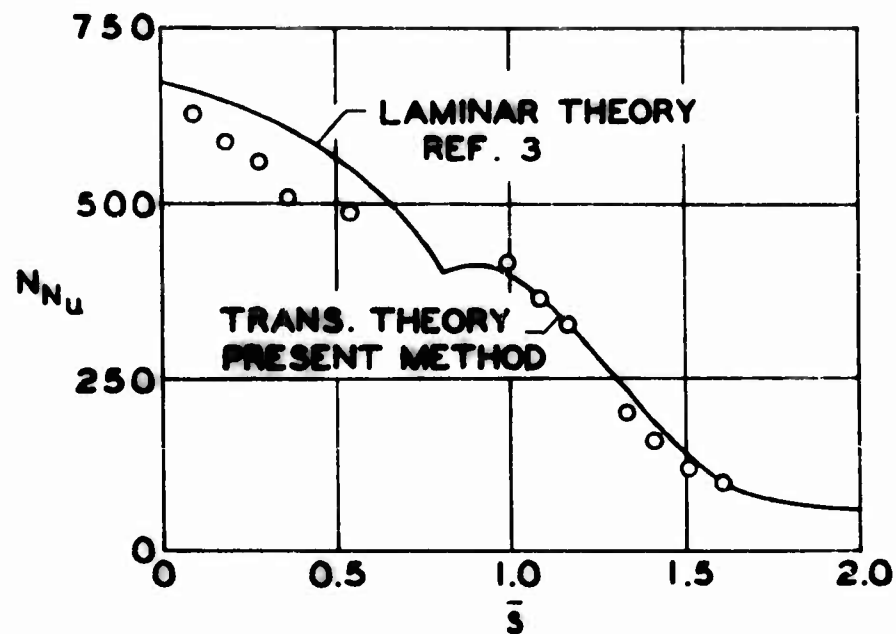
FIG. 22 DISTRIBUTION OF NUSSELT NUMBER
ON CALORIMETER. RUN NO. 4 $N_R = 1.20 \times 10^6$
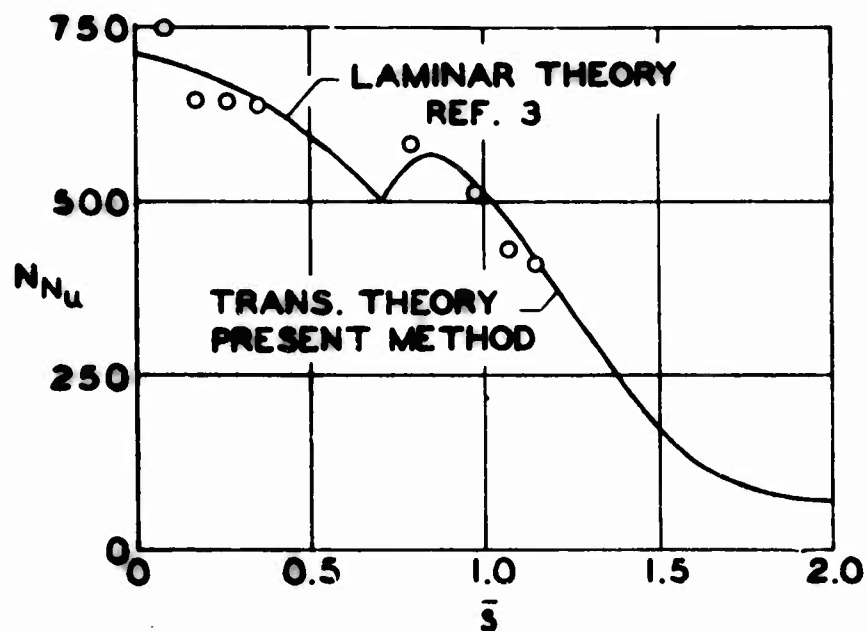
FIG. 23 DISTRIBUTION OF NUSSELT NUMBER
ON CALORIMETER. RUN NO. 5 $N_R = 1.35 \times 10^6$
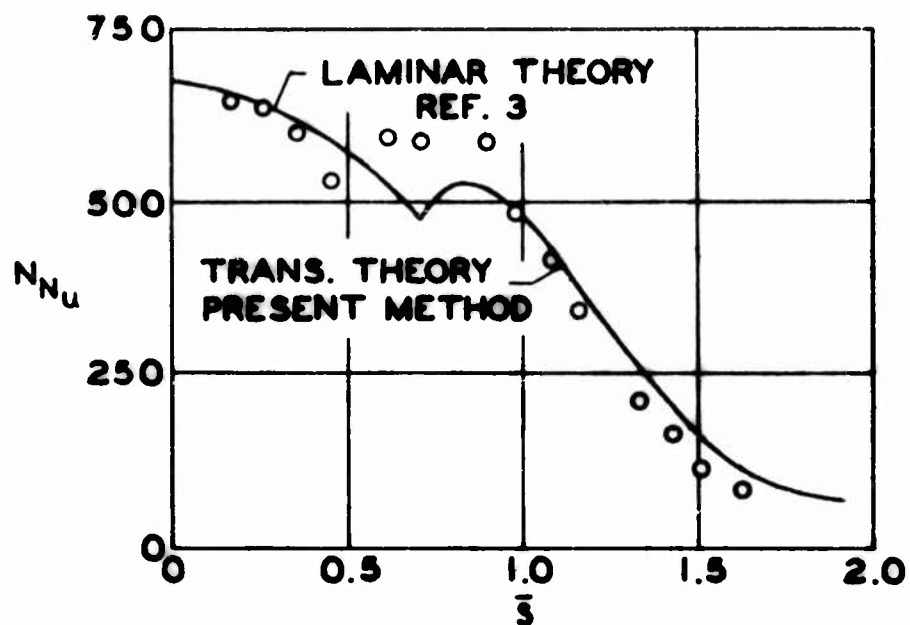
FIG. 24 DISTRIBUTION OF NUSSELT NUMBER
ON CALORIMETER. RUN NO. 6 $N_R = 1.24 \times 10^6$
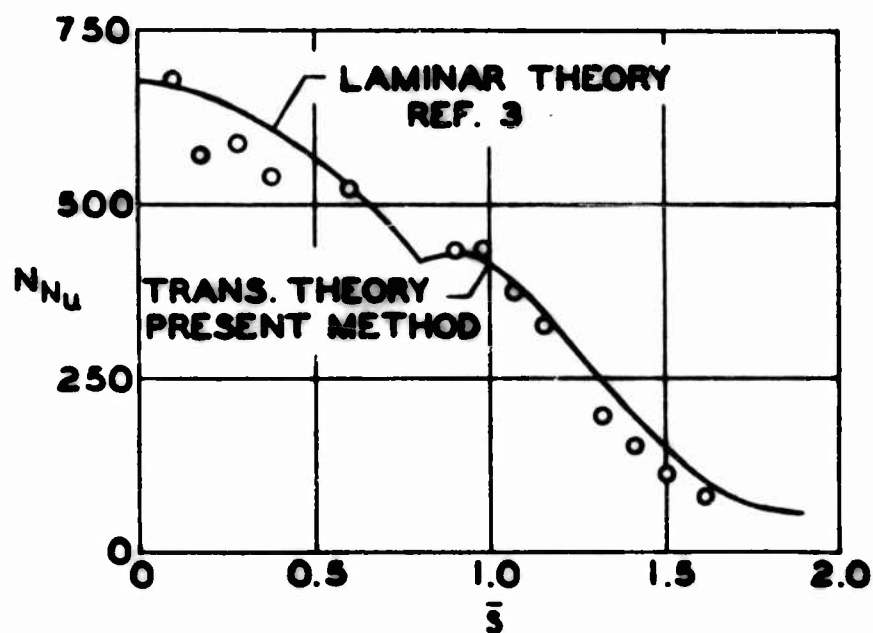
FIG. 25 DISTRIBUTION OF NUSSELT NUMBER
ON CALORIMETER. RUN NO. 7 $N_R = 1.24 \times 10^6$
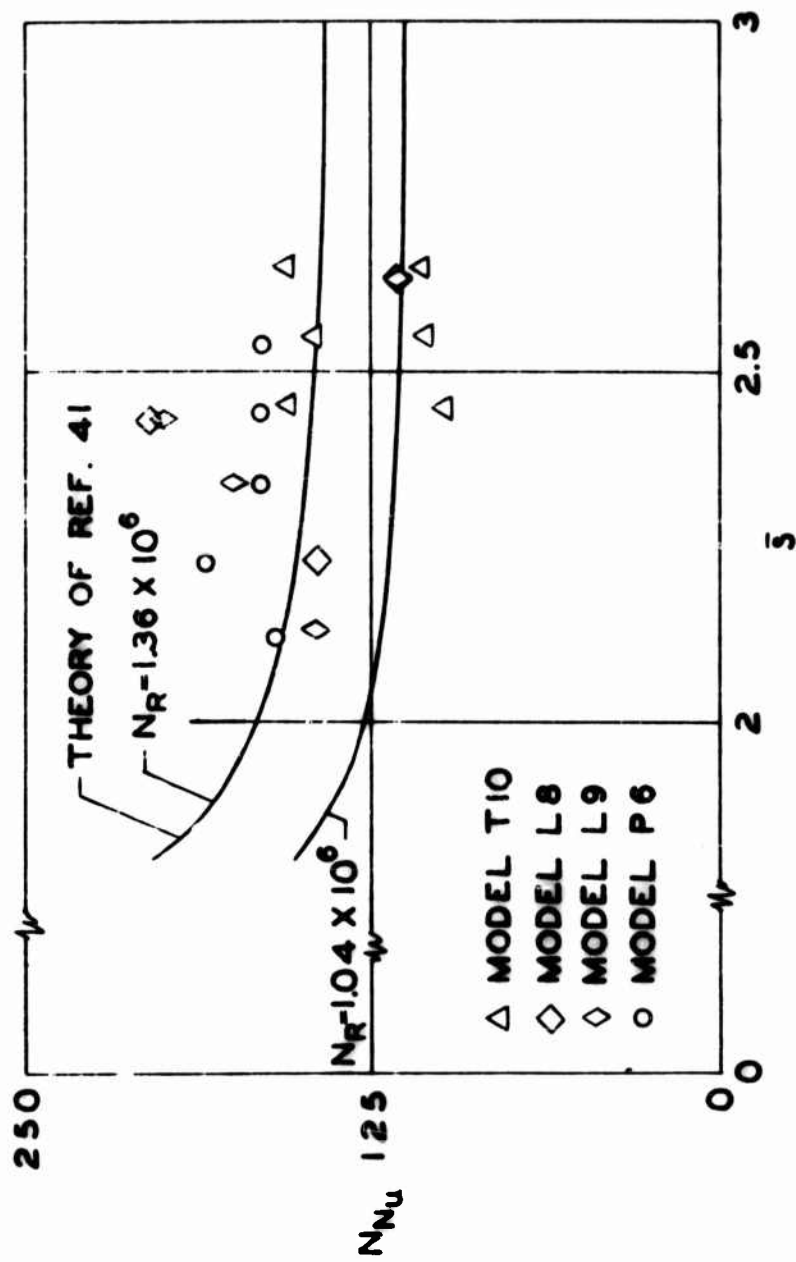
FIG. 26 TYPICAL DISTRIBUTIONS OF NUSSELT NUMBER
ON CYLINDRICAL SKIRT

an axisymmetric manner. The results of these measurements are presented in Figs. 27-34 in absolute terms and in a normalized form (percent of stagnation point ablation).

The total time of exposure t_t was read from both the films and the temperature traces and it is assumed that the total surface recession s_t which was measured corresponds to this time interval; that is, for $t > t_t$ no removal of material occurs.

The temperature histories obtained from the thermocouples located below the surface are presented in a semi-logarithmic plot in Figs 35-39. As has been noted in Section II, by presenting the data in this form the steady, linear variation of the temperature history may be observed from which an experimental determination of the quantity $B^2/\varkappa$ is obtained.

We may note at this time that since the steady mass ablation rate m was not determined, it is not possible to calculate the experimental values of h_{eff} for the various materials. Because of the initial transient period, the quantity s_t/t_t is less than B, since $ds/dt \leq B$. Evidently, the greater the period of unsteady ablation, the greater will be the difference between these two quantities. For a qualitative comparison between the various materials a rough value of h_{eff} has been calculated for the stagnation point where the transient period is a minimum in most cases by taking the measured ratio s_t/t_t as being equivalent to the steady ablation velocity. These values are included in Table II.

Photographs of the final configuration of the models superimposed on a silhouette of the original unablated models may be found in Figs. 40-43.
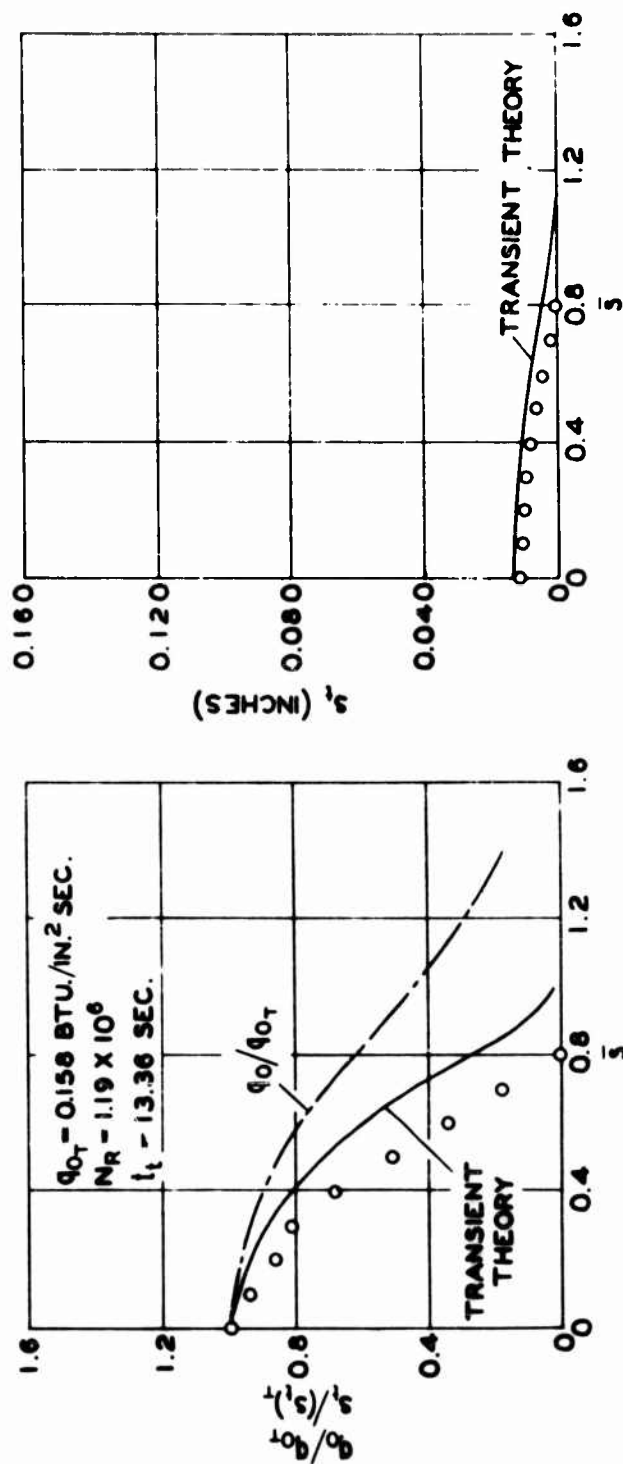
FIG. 27 DISTRIBUTION OF TOTAL ABLATION s_t - MODEL T5
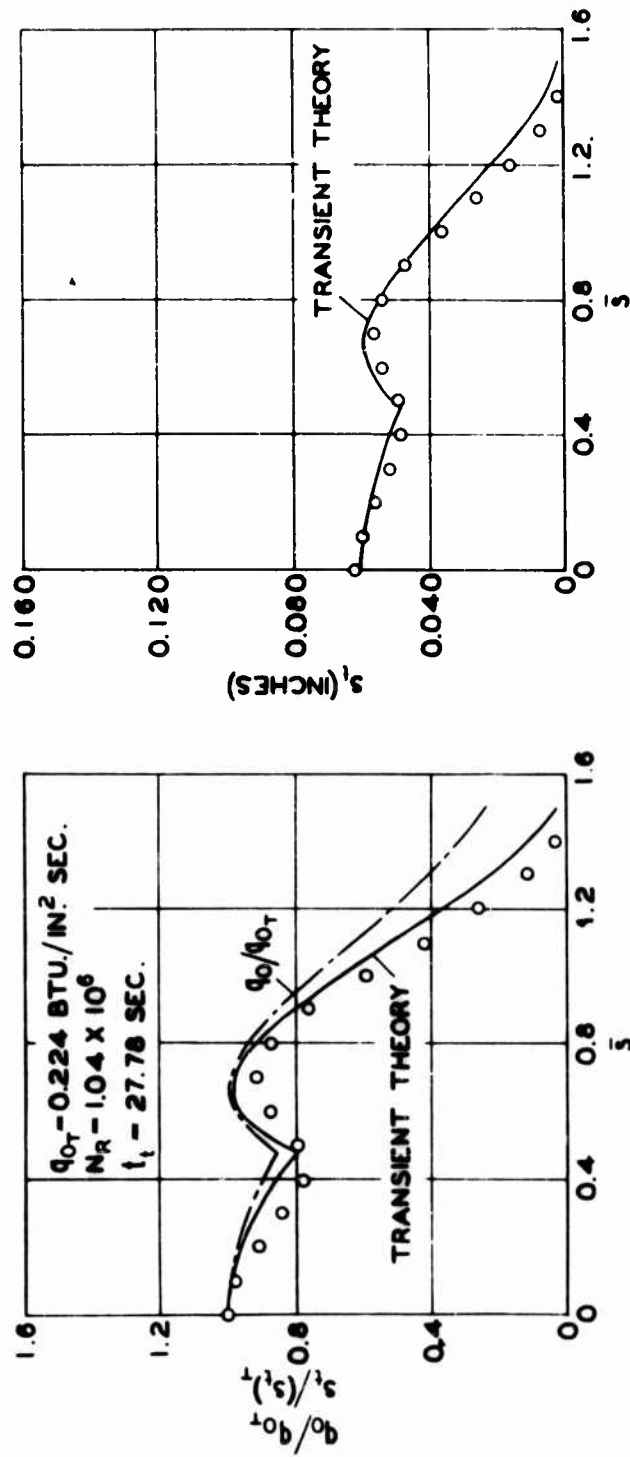
FIG. 28 DISTRIBUTION OF TOTAL ABLATION s_t – MODEL T 10
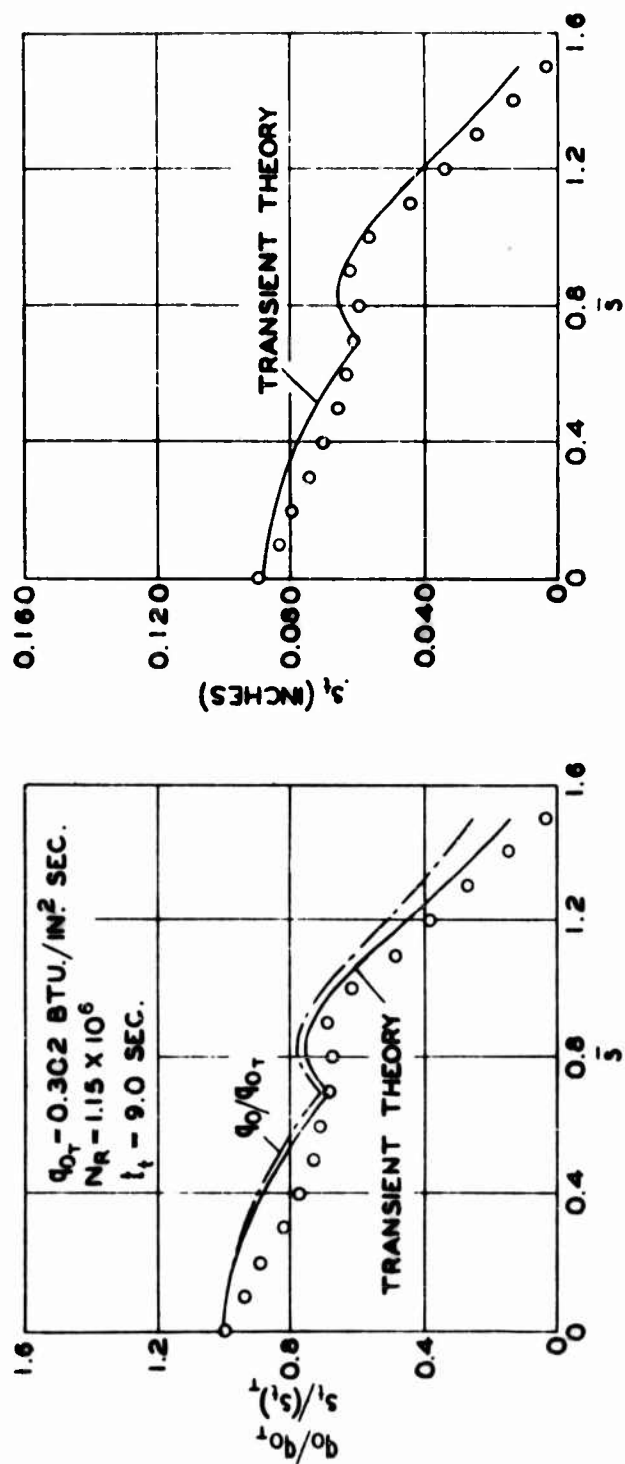
FIG. 29 DISTRIBUTION OF TOTAL ABLATION s_t — MODEL L8
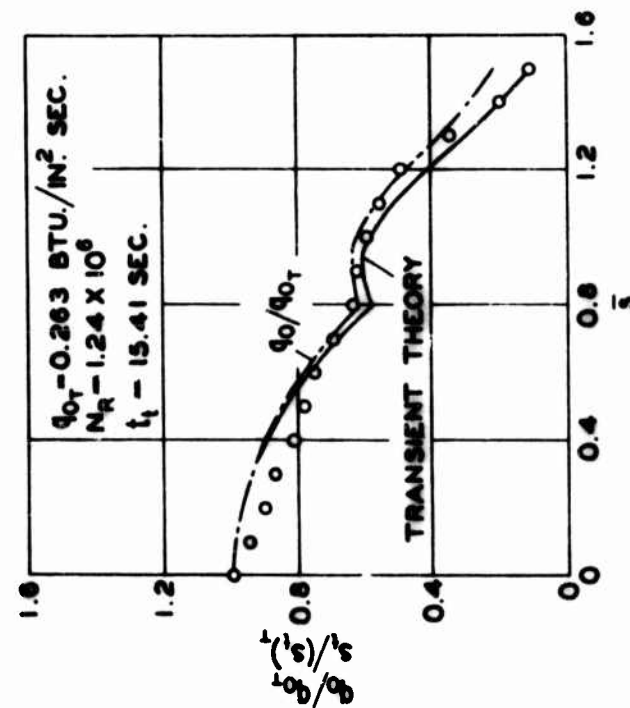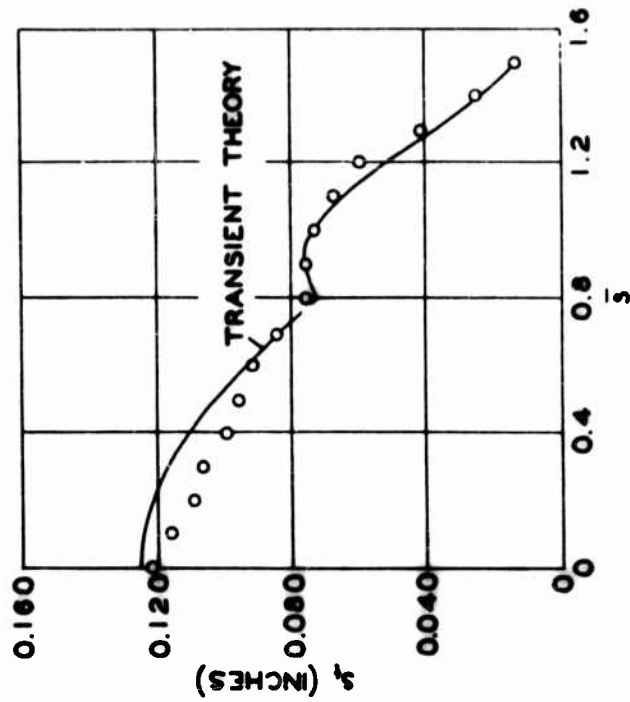
FIG. 30   DISTRIBUTION OF TOTAL ABLATION s_t – MODEL L9
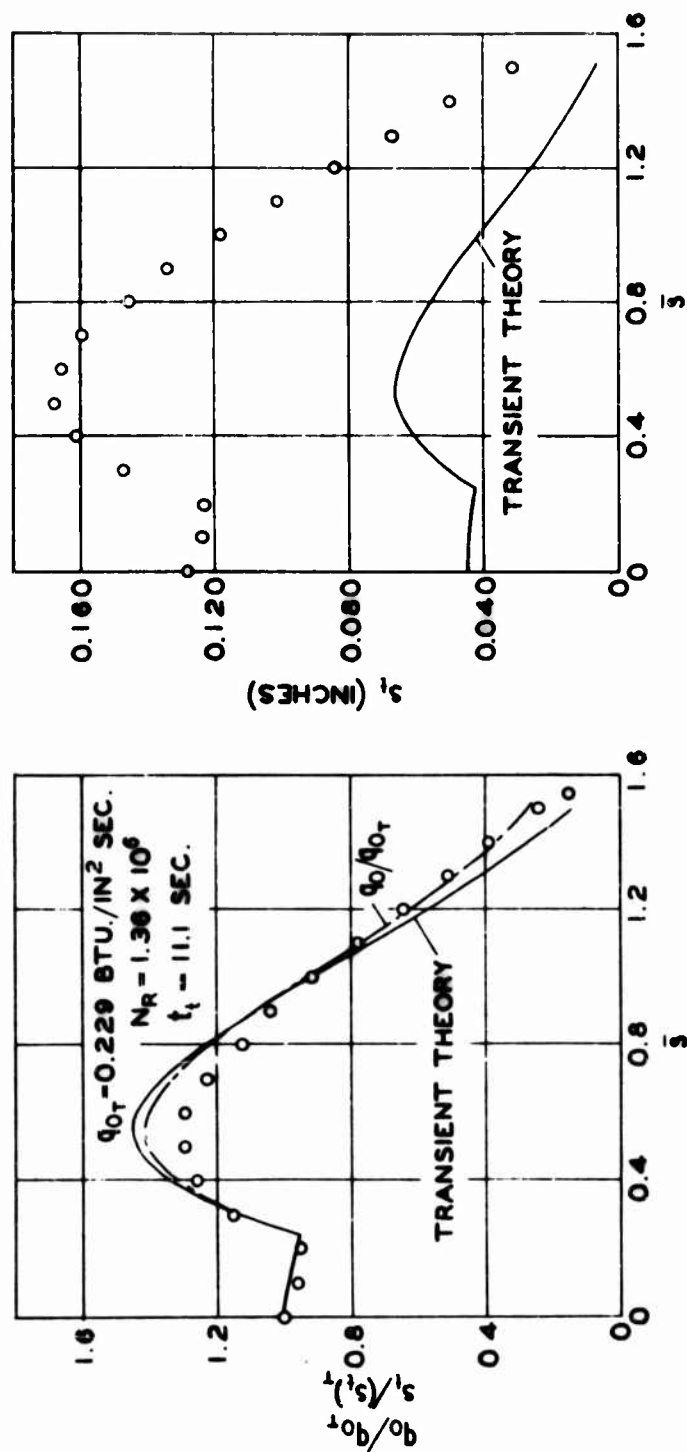
FIG. 31   DISTRIBUTION OF TOTAL ABLATION s_t - MODEL P2
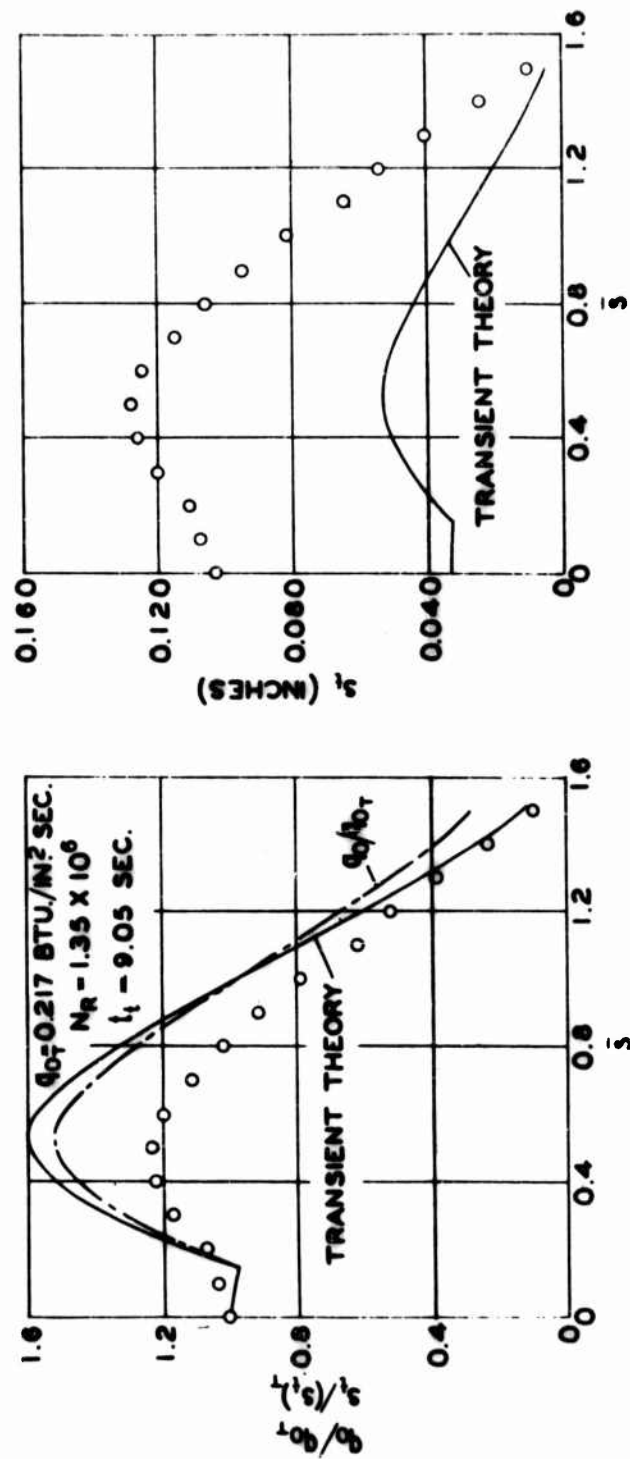
FIG. 32   DISTRIBUTION OF TOTAL ABLATION s_t – MODEL P6
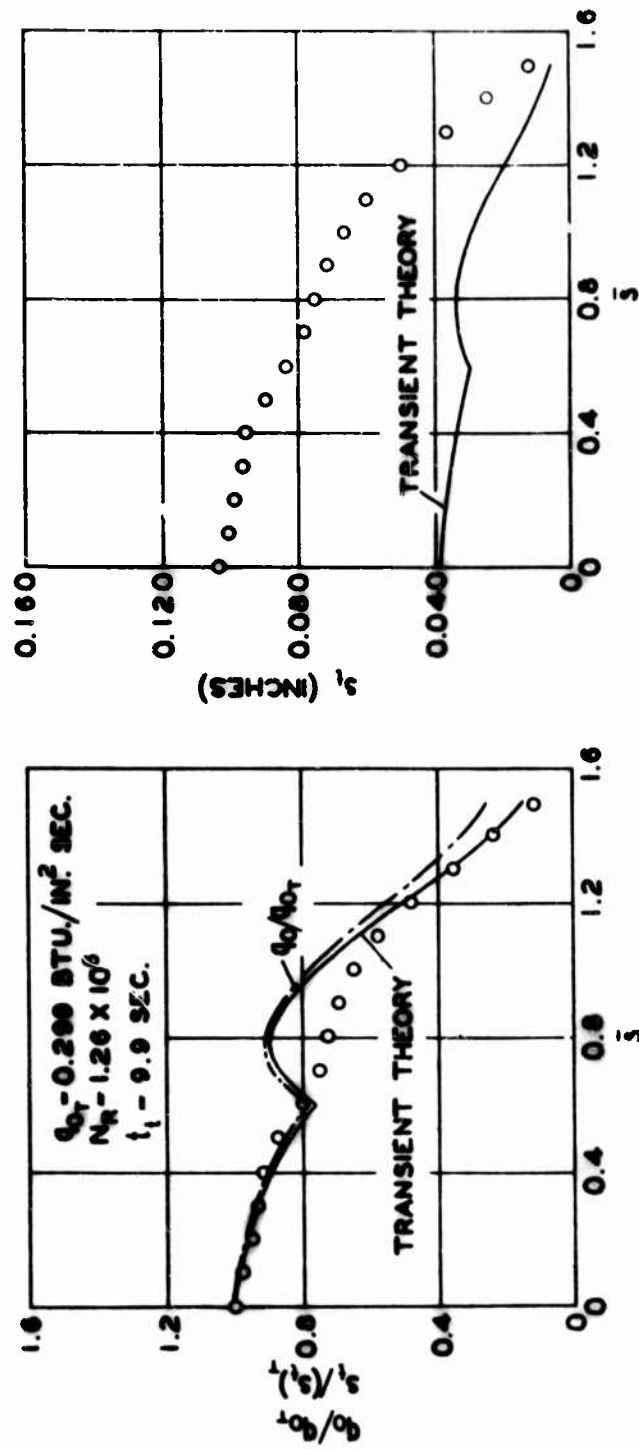
FIG. 33 DISTRIBUTION OF TOTAL ABLATION s_t - MODEL N3
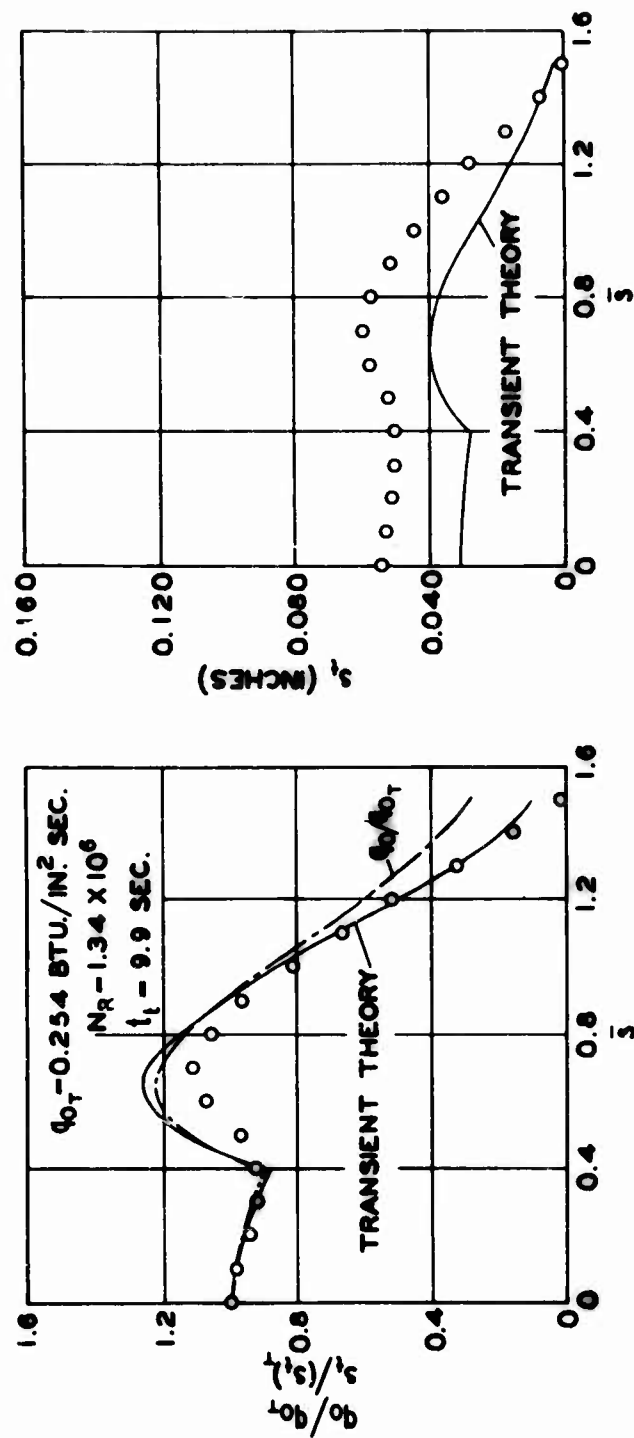
FIG. 34   DISTRIBUTION OF TOTAL ABLATION s_t – MODEL N7
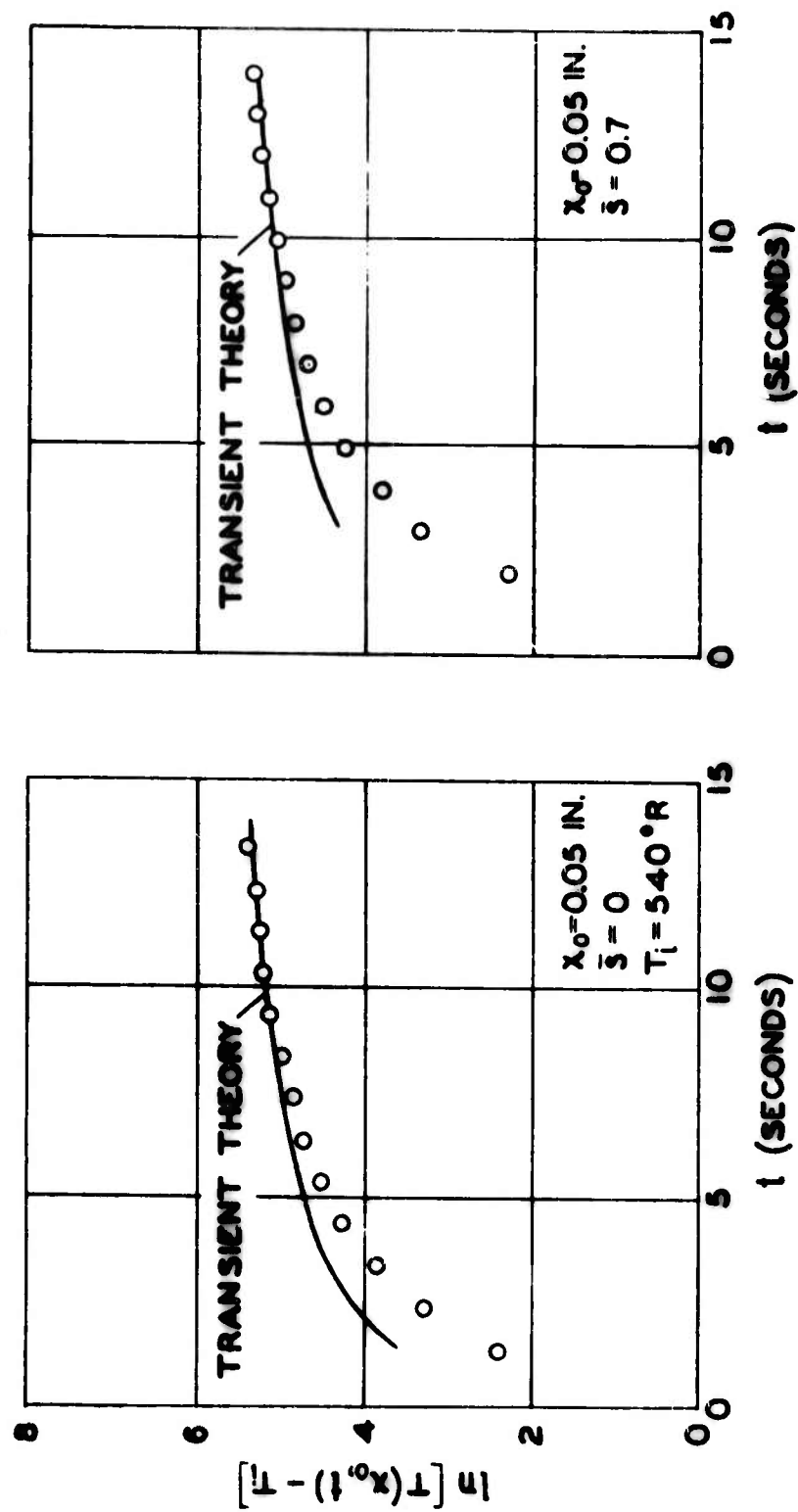
FIG. 35   TEMPERATURE HISTORY BELOW ABLATING SURFACE - MODEL T 5
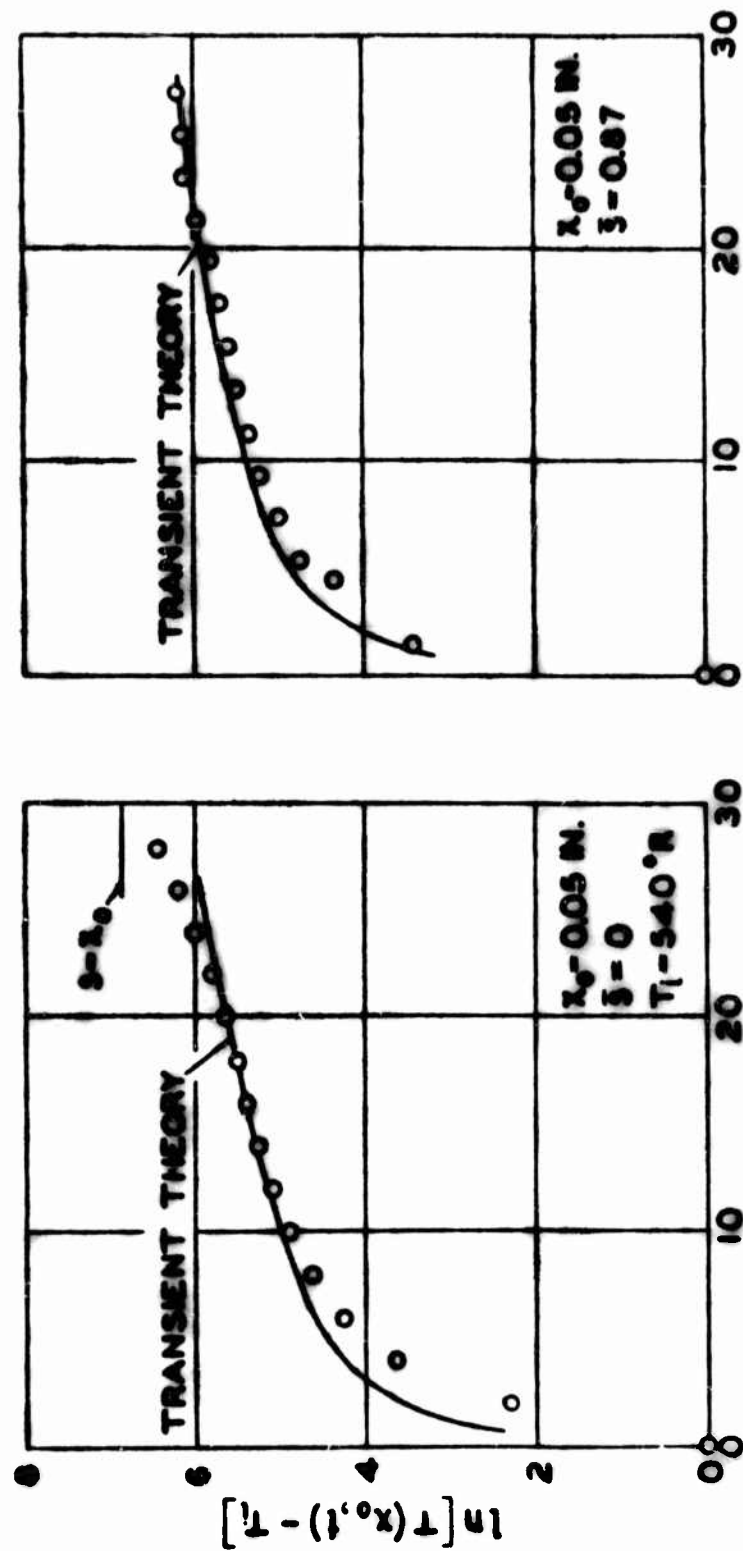
FIG. 36   TEMPERATURE HISTORY BELOW ABLATING SURFACE - MODEL T 10
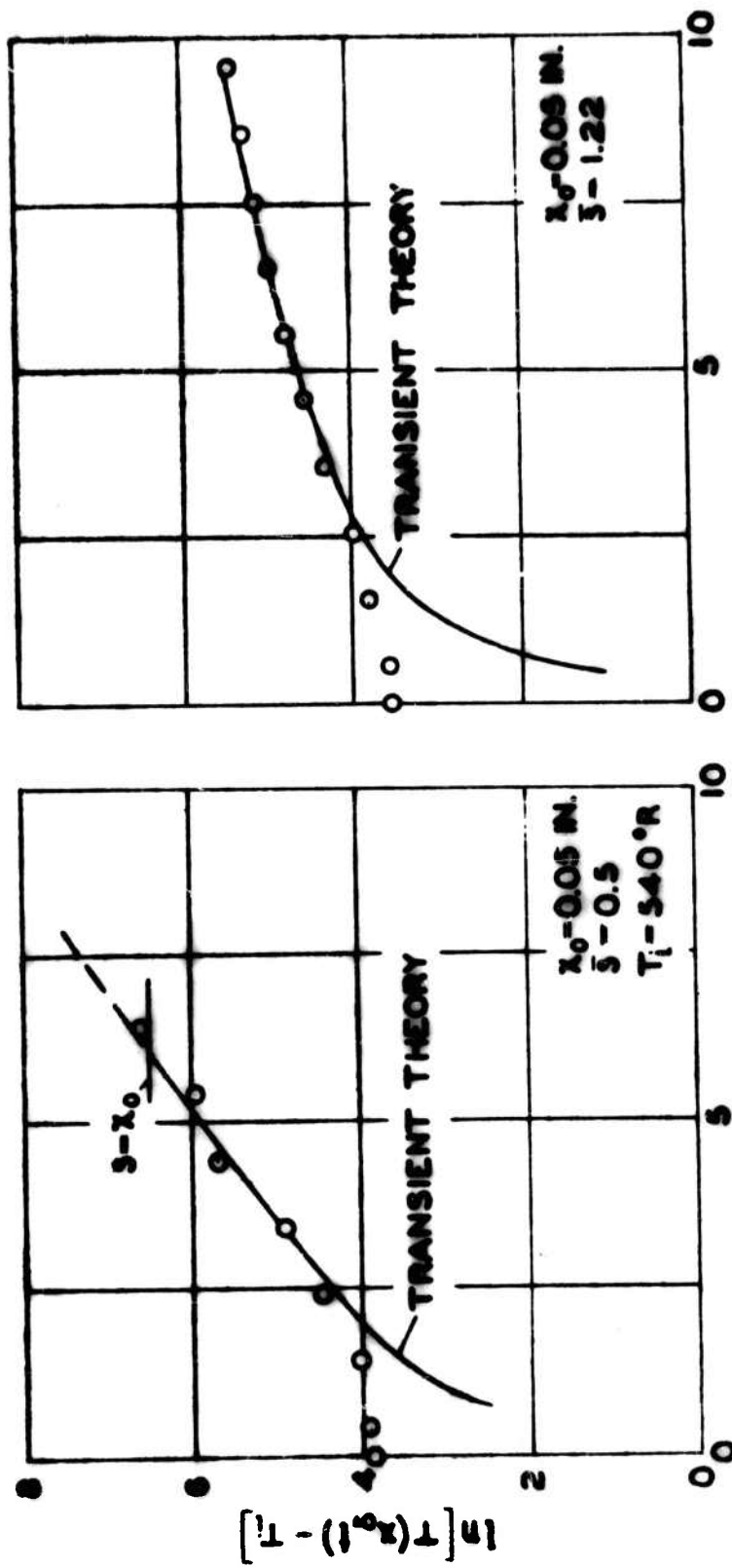
FIG. 37 TEMPERATURE HISTORY BELOW ABLATING SURFACE - MODEL L8
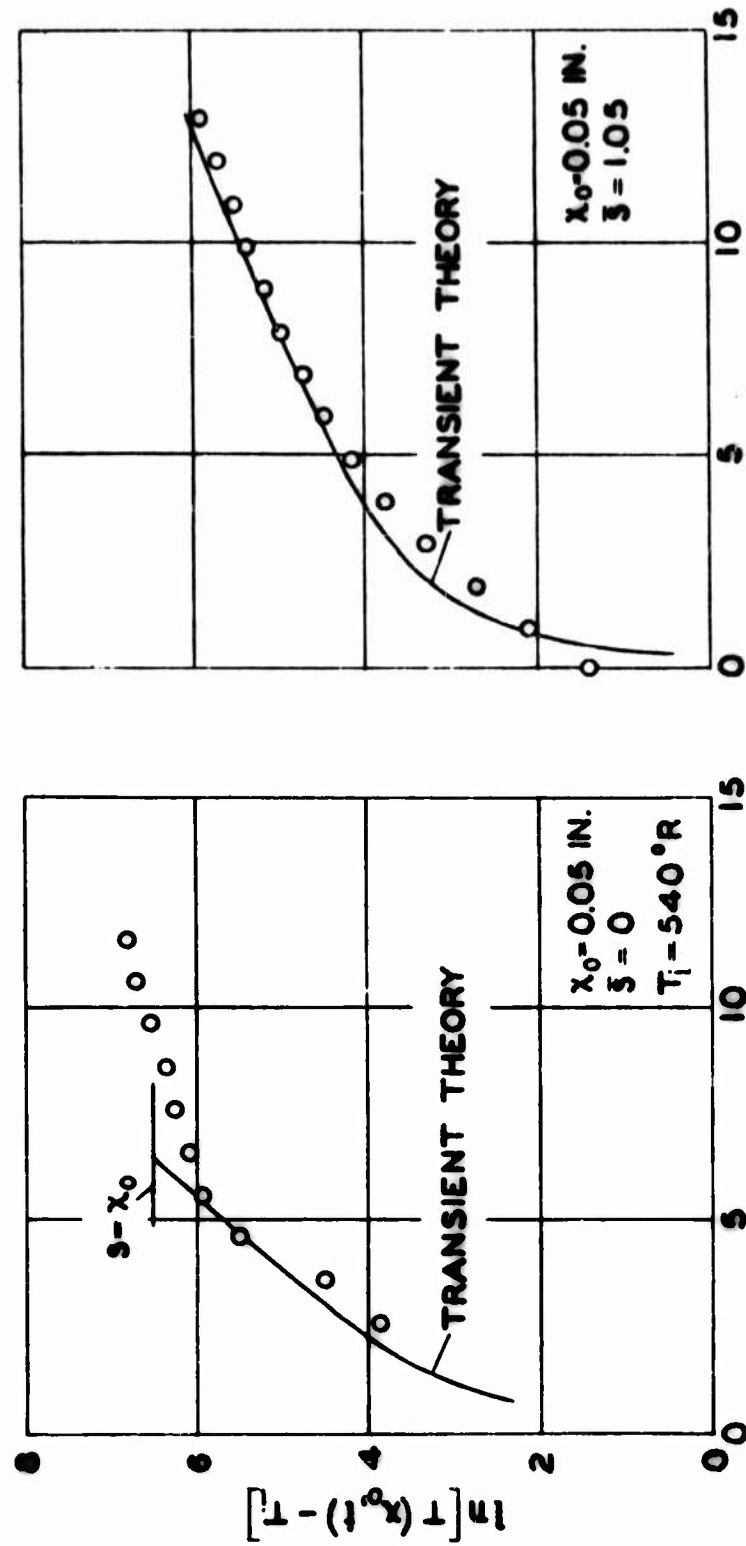
FIG. 38 TEMPERATURE HISTORY BELOW ABLATING SURFACE - MODEL L9
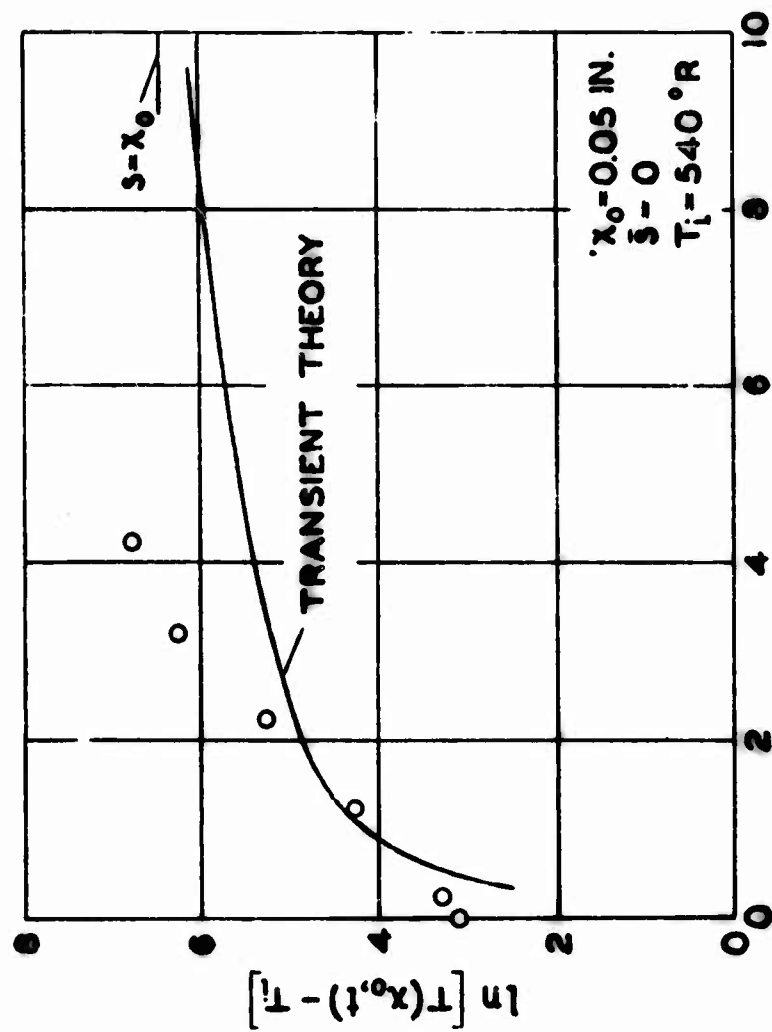
FIG. 39   TEMPERATURE HISTORY BELOW ABLATING
SURFACE - MODEL P6
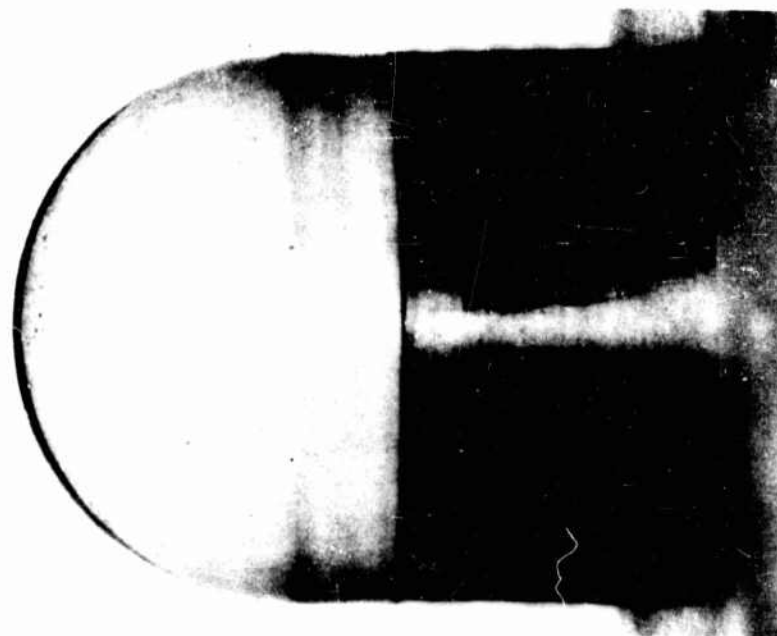
MODEL T10
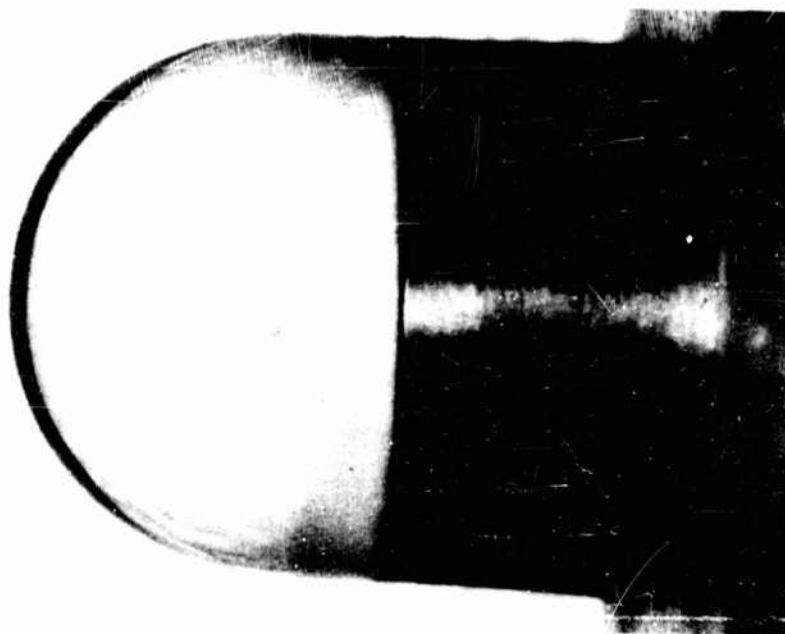
MODEL T5

FIG. 40. FINAL CONFIGURATION OF ABLATED MODELS
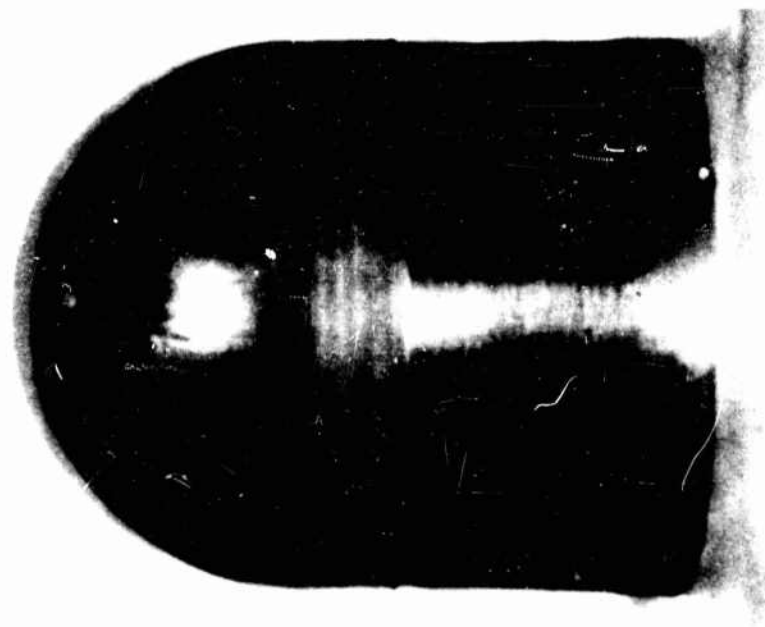
MODEL L9
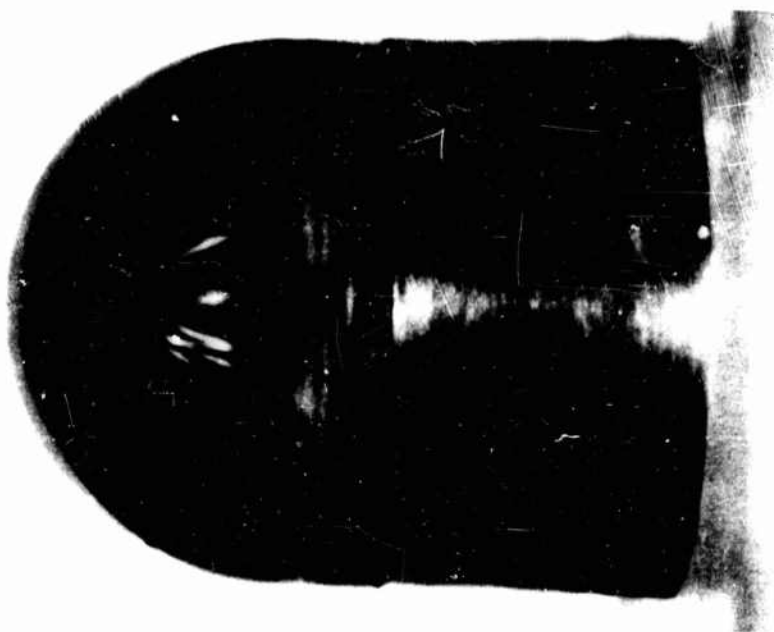
MODEL L8

FIG. 41. FINAL CONFIGURATION OF ABLATED MODELS
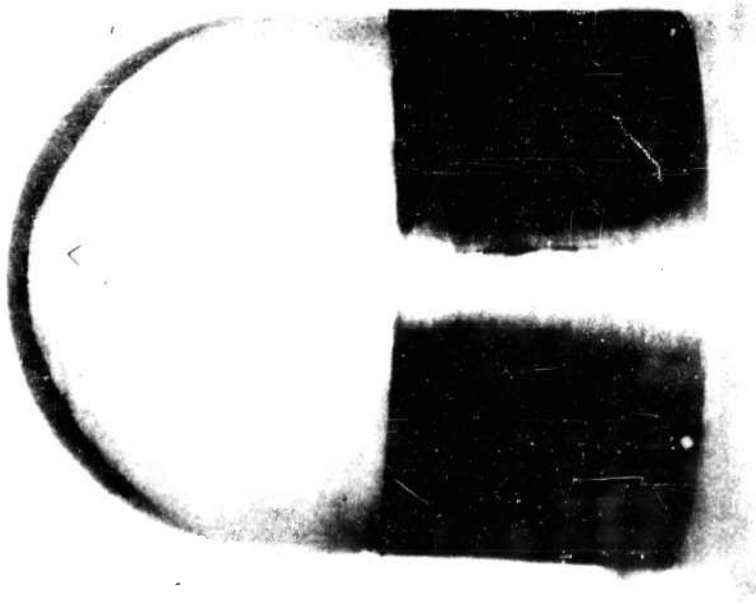
MODEL P6
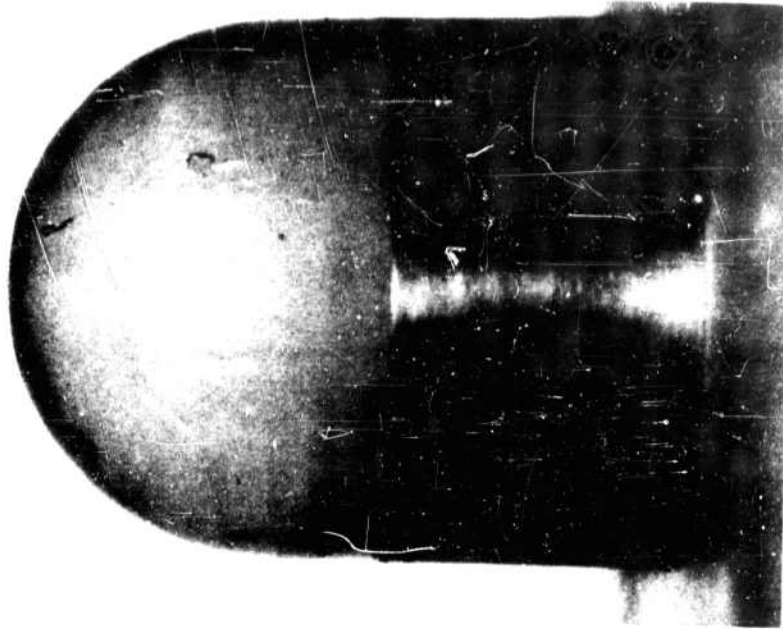
MODEL P2

FIG. 42. FINAL CONFIGURATION OF ABLATED MODELS
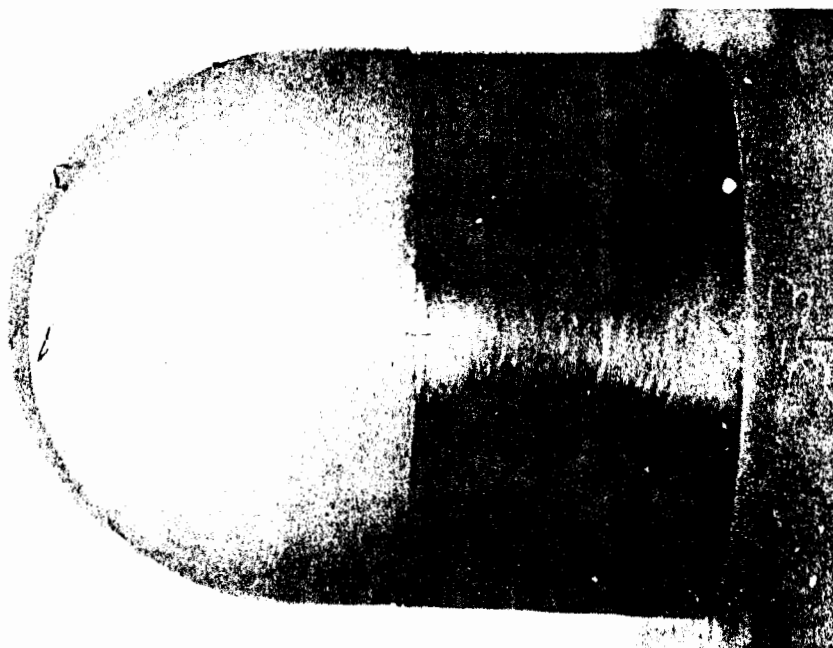
MODEL N7
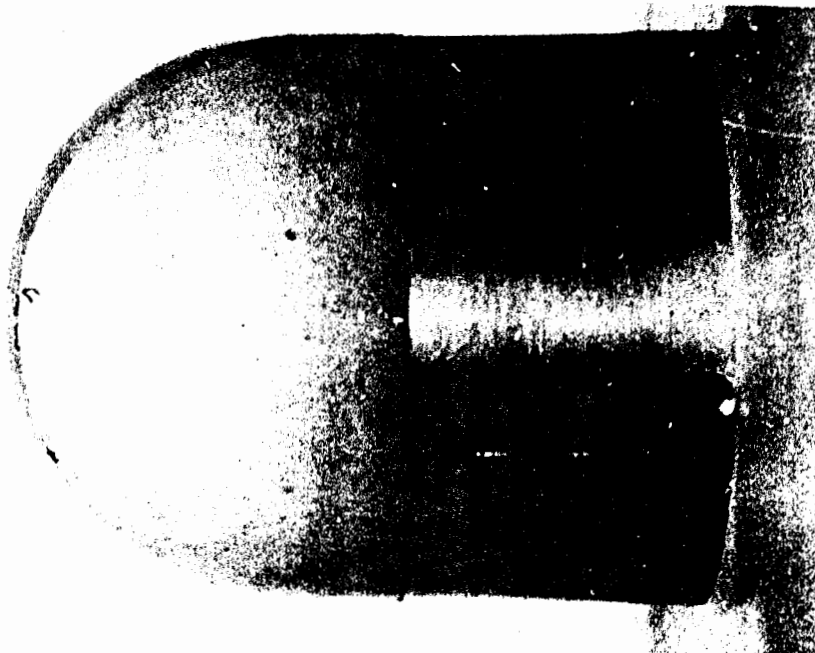
MODEL N3

FIG. 43. FINAL CONFIGURATION OF ABLATED MODELS

VI. COMPARISON WITH THEORY AND DISCUSSION OF RESULTS

A. Heat Transfer Rates from the Calorimeter Models

Inspection of the data presented in Figs. 22-25 indicates the possible existence of transitional heat transfer on the downstream portions of the calorimeter. In order to affect a comparison with theoretical predictions the location of transition was estimated from these plots.[*] Then, based on the pressure distribution of Fig. 17, the transitional theory described previously was utilized to obtain the corresponding distribution of N_{Nu} The resulting theoretical calculations of the combined laminar and transitional distribution are in reasonable agreement with the experimental data as can be seen in Figs. 22-25. It is interesting to note that for Run No. 5 with $N_R = 1.47 \times 10^6$ transition occurs approximately at a value of $\bar{s} = 0.7$ whereas for Run No. 4 with $N_R = 1.20 \times 10^6$ transition occurs further downstream at a value of $\bar{s} = 0.8$. The corresponding values of N_{R_θ} are approximately equal and have the value of 230. This is somewhat lower than the criterion for transition which was cited previously.

B. Ablation

For any particular ablation run the tunnel conditions and the physical properties of the model are specified, and hence **Eqs. (24) and (25)** may be utilized to obtain the theoretical variation of the surface recession and temperature (at a specified depth) with time. In particular, there may be computed $s_t = s(t_t)$ for several points on the hemisphere; these values will of course differ because of the different values of the aerodynamic heat flux q_o which exist at these points. Evidently, in order to carry out the calculation the distribution of q_o must be specified. It has been already shown that this distribution will probably be transitional in character and therefore highly sensitive to the particular flow Reynolds number which exists. Since, in general, the Reynolds number of any particular test was not equal to those obtained in the calorimeter runs, the following approach was adopted for determining the appropriate heat transfer rate distributions: From inspection of the data in Figs. 27-34, a transition point was estimated; the heat transfer distribution was then computed in a manner exactly analogous to that described previously. These distributions are included in Figs. 27-34 in a

---

[*]Actually, several different values were used until "best fit" of the data was obtained.

normalized form and are used to carry out the numerical calculation of the transient ablation theory. Qualitatively at least, we note that the final configuration of all models corresponds rather well to the assumed q_o distribution; i.e., the greatest removal of material occurs at stations where the heating is a maximum. In some cases of course, good quantitative agreement is also in evidence as, for example, for models T10 and L8.

Before proceeding to a discussion of the results and the comparison with the theoretical predictions it is necessary to make some comments concerning the properties of the various plastics which were tested. In particular, the materials which were used fall into two classes: those which melt (Nylon and Polyethylene), and those which sublime (Teflon and Lucite). Thus the calculations must be carried out for this distinctly different behavior and the appropriate formulation as developed in Section II must be utilized.

For the subliming materials Eqs. (13), (24), and (25) are used to determine s_t and the temperature history $T(x_o, t)$ where x_o represents the depth at which the thermocouples were installed. Here the value of Π is given by Eq. (I-3) in Appendix I. The results are presented in Figs. 27-30 and 35-38. With the exception of model T5, the agreement with the experimental data is quite good, not only at the stagnation point but over the entire hemispherical surface. On the basis of these results it would appear that the vapor injection at the stagnation region did not influence to any significant degree the conditions on downstream portions of the model. The rather large discrepancies which are observed for the case of model T5 may be attributed to the very small amounts of materials which were ablated, with the consequent increase in any error due to the measuring technique used.

Consider now the temperature histories which are presented in Figs. 35-38. As may be seen in Fig. 2 at $t=t_s$ the Eqs. (6) and (13) give rise to a discontinuity in the temperature history at any given value of x. This behavior is of course due to the assumed form for the temperature profile. Thus it is inconsistent to compare the actual theoretical values of the temperature at any time with those obtained experimentally. However, it is consistent and of interest to compare the steady state slopes since the integral method which has been formulated does yield the exact value of this slope, as has been indicated previously. In Figs. 35-38 this comparison is shown where, for convenience, the theoretical curve has been shifted parallel to the ordinate (i.e., downward) by an arbitrary amount. Again fairly good agreement is observed, particularly for models T5 and T10.

For the materials which vaporize, reaction of the vapor with the

constituents of the external boundary layer may occur. It has been indicated previously that such combustion will have a ngeligible effect for sufficiently high values of the driving enthalpy $h_\infty - h_s$. In the tests performed here this condition is not fulfilled, so that if combustion does occur, the ablation rates should be much greater than predicted by the transient theory to which the experimental results are compared. The results of this comparison would therefore indicate that combustion did not occur, either for the Teflon or Lucite models. The physical evidence available, though not conclusive, appears to verify this conclusion. No combustion is indiated either by the motion pictures of the test runs or by visual inspection of the ablated models.

Consider now the calculations for the melting materials. These are carried out as before, except that now we set $\Pi=0$ in Eqs. (14) and (20). The results of these calculations (see Figs. 31-34) yield values for the total surface recession s_t which are very much less than those actually experienced by the ablating models. This result is surprising in view of the conservative nature of the melting analysis which has been utilized (see Section II). One would expect this theory to overestimate the amount of material removed, particularly at the stagnation point where no build-up of liquid and consequent solidification can occur.

One possible explanation for this behavior is that the values of the physical constants used for nylon and polyethylene are in error. In general, the problem of obtaining reliable data on the properties of ablating materials is difficult. Of all of the data which has been obtained for use in these experiments the most doubtful were the latent heat of fusion L and the melting temperature T_m for the above-named materials.* Calculations indicate that the value of s_t is indeed sensitive to these parameters. (It is also sensitive to q_0 to the same degree, but in view of the consistent results obtained for the subliming cases there is no reason to suppose that the discrepancy is due to the use of unrealistic values of the heat flux rates). By adjusting the values of L and T_m an attempt to fit the experimental data was made. It was found that a unique set of values for these parameters could be obtained which, when combined with the transient theory, gave reasonable

---

* We may note, for example, that one source (reference 50) gives for the melting temperature of nylon a value which is higher than the stagnation temperature to which the nylon specimens were exposed in this investigation. This would indicate that no ablation should occur. Nevertheless, a considerable amount of material was removed, and this removal was evidently not a mechanical one as could be seen by visual inspection of the ablated models.

agreement with the experimental results for both tests of each material. These calculations are not presented since it is felt that the quantity of data available is insufficient to justify any definite conclusions.

In view of the possible inaccurate knowledge of the physical parameters, only one plot of the temperature history is presented and compared with the theoretically predicted values (see Fig. 39). Again the discrepancy is evident and indicates the same qualitative trend; that is, the theory gives a more shallow slope which corresponds to a lower value of the steady-state ablation rate. This behavior is observed in all cases for the melting materials.

VII. CONCLUDING REMARKS

An experimental and theoretical investigation of the transient ablation of plastic models in a hypersonic wind tunnel has been carried out. The existing theoretical studies of ablation have been reviewed. The approximate analysis of Goodman has been modified to include the interaction between the vaporizing material and the external boundary layer.

An experimental rig permitting tests in a free jet at a Mach number of 4.4 has been designed, constructed and connected to the pebble bed heater of the PIBAL hypersonic facility.

The models tested were hemispherical with a diameter of three inches. The models were instrumented with thermocouples initially below the surface and were observed photographically during exposure to the air stream. A calorimeter model was tested so as to provide the heat transfer without mass transfer. Laminar and transitional heat transfer were found to exist on the models; as an interesting result of the study it was found that the existing theories for transitional heat transfer under hypersonic conditions could be simply modified to provide better agreement between theory and these and other experiments.

The predicted total mass removed and the steady state ablation rates were found to be in good agreement with the measured data for the subliming materials (Teflon and Lucite). However, for the materials which melted, the material removed was found to be considerably less than

that predicted by the analysis. There are indications that this discrepancy is due to a lack of satisfactory knowledge of the physico-chemical properties of the materials.

VIII. REFERENCES

1. Lindemann, F. A. and Dobson, G. M. B.: Theory of Meteors and Density and Temperature of the Outer Atmosphere to Which it Leads. Proceedings of the Royal Society of London, Ser. A., Vol. 102, pp. 411-439, 1923.

2. Opik, E.: Atomic Collisions and Radiation of Meteors. Harvard Reprints No. 100, 1933.

3. Lees, L.: Laminar Heat Transfer Over Blunt-Nosed Bodies at Hypersonic Flight Speeds. Jet Propulsion, Vol. 26, No. 4, pp. 259-269, April 1956.

4. Cresci, R. J., MacKenzie, D. A., and Libby, P. A.: An Investigation of Laminar, Transitional and Turbulent Heat Transfer on Blunt-Nosed Bodies in Hypersonic Flow. Polytechnic Institute of Brooklyn, PIBAL Report No. 466, WADC TN 59-119. AD 214 617, April 1959.

5. Evans, G. W., Isaacson, E., and MacDonald, J. K. L.: Stefan-Like Problems. Quarterly of Applied Mathematics, Vol. 8, pp. 312-319, 1950.

6. Cheng, S.: On the Mechanisms of Atmospheric Ablation. Presented at the IXth International Astronautical Congress, Amsterdam, August 1958.

7. Landau, H. G.: Heat Conduction in a Melting Solid. Quarterly of Applied Mathematics, Vol. 8, pp. 81-94, April 1950.

8. Goodman, T. R.: Aerodynamic Ablation of Melting Bodies. Proceedings of the Third U.S. National Congress of Applied Mechanics, Brown University, 1958.

9. Citron, S. J.: <u>Heat Conduction in a Melting Slab.</u> Presented at the Institute of Aeronautical Sciences 27th Annual Meeting, New York, January 1959.

10. Sutton, G. W.: <u>The Hydrodynamics and Heat Conduction of a Melting Surface.</u> Journal of the Aeronautical Sciences, Vol. 25, No. 1, pp. 29-32, January 1958.

11. Lees, L.: <u>Similarity Parameters for Surface Melting of a Blunt-Nosed Body in a High Velocity Gas Stream.</u> American Rocket Society Journal, Vol. 29, No. 5, pp. 345-354, May 1959.

12. Bethe, H. A. and Adams, Mac C.: <u>A Theory for the Ablation of Glassy Materials.</u> Journal of the Aero/Space Sciences, Vol. 26, No. 6, pp. 321-328, June 1959.

13. Roberts, L.: <u>A Theoretical Study of Stagnation-Point Ablation.</u> NACA TN 4392, September 1958.

14. Georgiev, S., Hidalgo, H., and Adams, Mac C.: <u>On Ablation for the Recovery of Satellites.</u> AVCO-Everett Research Laboratory, Research Report 47, March 1959.

15. Bonin, J. H., Price, C. F., and Taylor, D. E.: <u>Determination of Factors Governing Selection and Application of Materials for Ablation Cooling of Hypervelocity Vehicles.</u> Chicago Midway Laboratories, The University of Chicago, WADC TR 59-87, January 1959.

16. Bond, A. C., Rashis, B., and Levin, L. R.: <u>Experimental Ablation Cooling.</u> NACA RM L58E15a, July 1958.

17. Scala, S. M.: <u>The Thermal Protection of a Reentry Satellite.</u> General Electric Rep. R59SD336, March 1959.

18. Scala, S. M.: <u>A Study of Hypersonic Ablation.</u> General Electric Company, T.I.S. Document No. R59SD438, September 1959.

19. Georgiev, S., Hidalgo, H., and Adams, Mac C.: <u>On Ablating Heat Shields for Satellite Recovery.</u> AVCO-Everett Research Laboratory, Research Note 147, July 1959.

20. Scala, S. M.: <u>The Thermal Degradation of Reinforced Plastics During Hypersonic Re-Entry.</u> General Electric Company, T.I.S. Document No. R59SD401, July 1959.

21. Diaconis, N., Fanucci, J., and Sutton, G. W.: The Heat Protection Potential of Several Ablation Materials for Satellite and Ballistic Re-Entry into the Earth's Atmosphere. Fourth Symposium on Ballistic Missile and Space Technology, Space Technology Laboratories, California, August 1959.

22. Scala, S. M. and Sutton, G. W.: The Two-Phase Hypersonic Laminar Boundary Layer, A Study of Surface Melting. 1958 Heat Transfer and Fluid Mechanics Institute, University of California, June 1958.

23. Scala, S. M.: Transpiration Cooling in the Hypersonic Laminar Boundary Layer. (To be published).

24. Fanucci, J. B.: Ablation Characteristics of a Glassy Material in a Decelerating Environment. Aerophysics Technical Memorandum No. 135, General Electric Company (MSVD).

25. Adams, Mac C.: Recent Advances in Ablation. American Rocket Society Journal, Vol. 29, No. 9, pp. 625-632, September 1959.

26. Adams, Mac C., Powers, W. E., and Georgiev, S.: An Experimental and Theoretical Study of Quartz Ablation at the Stagnation Point. AVCO-Everett Research Laboratory, Research Report 57, June 1959.

27. Knuth, E. L.: Compressible Couette Flow With Diffusion of a Reactive Gas From a Decomposing Wall. 1958 Heat Transfer and Fluid Mechanics Institute, pp. 104-113, June 1958.

28. Dooley, D. and Denison, R.: Combustion in the Laminar Boundary Layer of Chemically Active Sublimators. Aeronutronics Systems Publication U-110, September 1957.

29. Sutton, G. W.: Adiabatic Wall Temperature Due to Mass Transfer Cooling with a Combustible Gas. Jet Propulsion, Vol. 29, No. 2, pp. 136-137, February 1958.

30. Sutton, G. W.: Combustion of a Gas Injected into a Hypersonic Laminar Boundary Layer. Proceedings of the Seventh International Combustion Symposium, Butterworths, London (1958).

31. Carslaw, H. S. and Jaeger, J. C.: Conduction of Heat in Solids, Oxford at the Clarendon Press, 1950.

32. Cresci, R. J. and Libby, P. A.: Some Heat Conduction Solutions Involved in Transient Heat Transfer Measurements. Polytechnic Institute of Brooklyn, PIBAL Report No. 384, WADC TN 57-236, AD 130 800, September 1957.

33. Pohlhausen, K.: Zur naherungsweisen Integration der Differential-gleichunger der Laminaren Grenzschiecht. Zeitschrift für angewandte Mathematik und Mechanik, Vol. 1, pp. 252-258, 1921.

34. Goodman, T. R.: The Heat-Balance Integral and Its Application to Problems Involving a Change of Phase. Presented at the Heat Transfer and Fluid Mechanics Institute, Pasadena, California, June 1957.

35. Sutton, G. W.: The Ablation of Reinforced Plastics in Supersonic Flow. General Electric Report AORM 3, No. 57SD644, July 1957.

36. Hartnett, J. P. and Eckert, E. R. G.: Mass Transfer Cooling with Combustion in a Laminar Boundary Layer. 1958 Heat Transfer and Fluid Mechanics Institute, pp. 54-68, June 1958.

37. Fay, J. A., Riddell, F. R., and Kemp, N. H.: Stagnation Point Heat Transfer in Dissociated Air Flow. Jet Propulsion, Vol. 27, No. 6, pp. 672-674, June 1957.

38. Anon.: Tables of Various Mach Number Functions for Specific Heat Ratios from 1.2 to 1.38. NACA TN 3981, April 1957.

39. Persh, J.: A Procedure for Calculating the Boundary Layer Development in the Region of Transition from Laminar to Turbulent Flow. U.S.N.O.L. NAVORD Report 4438, March 1957.

40. Vaglio-Laurin, R.: Turbulent Heat Transfer on Blunt-Nosed Bodies in Two-Dimensional and General Three-Dimensional Hypersonic Flow. Polytechnic Institute of Brooklyn, PIBAL Report No. 458, WADC TN 58-301, AD 206 050, September 1958.

41. Libby, P. A. and Cresci, R. J.: Evaluation of Several Hypersonic Turbulent Heat Transfer Analyses by Comparison with Experimental Data. Polytechnic Institute of Brooklyn, PIBAL Report No. 387, WADC TN 57-72, AD 118 093, July 1957.

42. Ferri, A. and Libby, P. A.: The Hypersonic Facility of the Polytechnic Institute of Brooklyn and Its Application to Problems of Hypersonic Flight. Polytechnic Institute of Brooklyn, PIBAL Report No. 392, WADC TR 57-369, AD 130 809, August 1957.

43. Zakkay, V.: Status Report of the Hypersonic Facility of the Polytechnic Institute of Brooklyn. PIBAL Report No. 602, April 1960.

44. Clippinger, R. F.: Supersonic Axially Symmetric Nozzles. Ballistic Research Laboratories Report No. 794, December 1951.

45. Ruptash, J.: Growth of Boundary Layer in Supersonic Nozzles. Presented at the First Symposium on High Speed Aerodynamics, National Aeronautical Establishment, Ottawa, Canada, February 1953.

46. Yu, Ying-Nien: A Summary of Design Technique for Axisymmetric Hypersonic Wind Tunnels. Agardograph 35, November 1958.

47. Stetson, K. F.: Boundary Layer Transition on Blunt Bodies with Highly Cooled Boundary Layers. Paper presented at the I.A.S. 27th Annual Meeting, New York, January 26-29, I.A.S. Report No. 59-36.

48. Casaccio, A.: Theoretical Pressure Distribution on a Hemisphere-Cylinder Combination. Journal of the Aero/Space Sciences, Vol. 26, No. 1, pp. 63-64, January 1959.

49. Zakkay, V.: Pressure and Laminar Heat Transfer Results in Three-Dimensional Hypersonic Flow. Polytechnic Institute of Brooklyn, PIBAL Report No. 447, WADC TN 58-182, AD 155 679, September 1958.

50. Wood, R. M. and Tagliani, R. J.: Heat Protection by Ablation. Aero/Space Engineering, Vol. 19, No. 7, pp. 32-38, 45, July 1960.

51. Gross, J. J., Masson, D. J., and Gazley, C. Jr.: General Characteristics of Binary Boundary Layers with Applications to Sublimation Cooling. Rand Report P-1371, May 1958.

52. Stewart, J. D.: Transpiration Cooling: An Engineering Approach. General Electric Report MSVD-TIS-R59SD338, May 1959.

53.   Leadon, B. M. and Scott, C. J.: Mass Transfer Cooling at Mach
       Number 4.8. Journal of the Aeronautical Sciences, Vol. 25, No. 1,
       pp. 67-68, January 1958.

54.   Pappas, C. C.: Effect of Injection of Foreign Gases on the Skin
       Friction and Heat Transfer of the Turbulent Boundary Layer. IAS
       Report 59-78, January 1959.

55.   Myers, H.: Aerodynamically Heated Surfaces - A Chemical Analysis.
       Aero/Space Engineering, Vol. 19, No. 2, pp. 34-38, 103, February
       1960.

56.   Libby, P. A. and Cresci, R. J.: Experimental Investigation of the
       Downstream Influence of Stagnation Point Mass Transfer. Polytechnic
       Institute of Brooklyn, PIBAL Report No. 520, WADC TN 59-210,
       September 1959.

APPENDIX I

DEPENDENCE OF HEAT FLUX ON ABLATION RATE

Eq. (14) indicates that the net heat flux to the surface decreases
linearly with the ablation rate.* This effect is exactly analogous to so-called
mass transfer cooling resulting from vapor injection into the boundary layer.
In this case the vapor injection is provided by the sublimation of the solid
material. Extensive investigation of this phenomenon (see, for example,
reference 51) has resulted in the following approximate correlation formula:

$$q = q_o - \frac{2}{3} M^{\frac{1}{4}} \rho \frac{ds}{dt} (h_\infty - h_w) \qquad (I-1)$$

Here q_o is the heat transfer rate to the surface in the absence of

---

* The ablation rate is actually $(\rho \frac{ds}{dt})$, but since the density of the plastics is
assumed constant in this analysis the distinction is irrelevant to the dis-
cussion here.

mass transfer (evaluated at the surface temperature T_w), M is the ratio of molecular weights of air to the injected gas, and $(h_\infty - h_w)$ represents the enthalpy difference across the boundary layer. The numerical factor $\frac{2}{3}$ is valid only for a laminar boundary layer, and would be significantly different for the turbulent case (see references 52, 53, and 54). These references indicate that the factor $\frac{2}{3}$ should be replaced by $\frac{2}{9}$.

If Eq. (I-1) is to be applied at an ablating surface, h_w and q_0 must be evaluated at the ablation temperature T_s, while ρ and M must correspond to the gas liberated by the ablation process. By virtue of the above considerations Eq. (14) becomes

$$ q(t) = q_0 \Big|_{T_s = T_w} - \frac{2}{3} M^{\frac{1}{4}} \rho (h_\infty - h_s) \frac{ds}{dt} \qquad (I-2) $$

so that

$$ \Pi \equiv \frac{2}{3} M^{\frac{1}{4}} \rho (h_\infty - h_s) \qquad (I-3) $$

It should be noted here that chemical reactions and re-radiation from the ablating surface are implicitly excluded by the expression for the heat balance at the interface [i.e., Eq. (9)]. For pure plastic materials (and in general for subliming types of materials), the neglect of radiation is justifiable, since the maximum surface temperatures will be relatively low. No such a priori justification exists for the neglect of chemical reactions. However, at least one investigator (reference 55) has found experimentally that no combustion takes place under hypersonic conditions. The experimental results obtained here also indicate the absence of any chemical reaction (see Section VI).

APPENDIX II

TEMPERATURE PROFILE

The temperature profile assumed in the previous analysis, in a slightly rearranged form, is

$$\frac{T(x,t)-T_i}{T_s-T_i} = \exp\left[-\frac{x-s}{\delta}\right]$$

(II-1)

$$s = s(t)$$

$$\delta = \delta(t)$$

The quantity δ has been referred to at times as the "e-folding" length (see reference 21), since at the distance $x = \delta + s$ from the origin the temperature is given by

$$\frac{T(\delta+s,t)-T_i}{T_s-T_i} = \frac{1}{e}$$

(II-2)

Of significance from the mathematical point of view is the fact that

(i) The profile of Eq. (II-1) approaches the exact profile for steady ablation for large time.

(ii) The profile does not satisfy exactly the initial conditions which are carried over from the "heat sink" portion of the problem [i.e., Eq. (12)].

With regard to (ii) above, the following may be noted. First, the profiles of Eq. (II-1) and of Eq. (6) give for $t=t_s$ identical temperature gradients at the surface, i.e.:

$$\frac{\partial T(0,t_s)}{\partial x} = -\frac{q_o}{k}$$

Second, the heat stored in the solid at this time as calculated by the two profiles differ roughly only by 25% [the exact profile (6) gives a lower value of stored energy] for the types of materials and the environment to which this analysis is applied. For example,

$$Q_{stored\ (exact)} = \int_0^\infty \rho c_p (T - T_i) dx$$

$$= \rho c_p (T_\infty - T_i) 2 Nu\ \frac{k}{h}\ \int_0^\infty erfc\ X - e^{Nu(Nu+2X)} erfc(Nu+X) dX$$

$$= \rho c_p (T_\infty - T_i) 2 Nu\ \frac{k}{h}\ [\frac{1}{\sqrt{\pi}} - \frac{1}{2 Nu} (1 - e^{Nu^2} erfc\ Nu)]$$

where, of course, Nu is evaluated at $t = t_s$.

On the other hand, for the approximate profile

$$Q_{stored\ (approx.)} = \int_0^\infty \rho c_p (T_s - T_i)\ exp[-\frac{x}{\delta(t_s)}] dx$$

$$= \rho c_p\ \frac{(T_s - T_i)^2}{(T_\infty - T_s)}\ \frac{k}{h}$$

The ratio is thus

$$\frac{Q_{st.\ ex.}}{Q_{st.\ app.}} = \frac{(T_\infty - T_i)(T_\infty - T_s)}{(T_s - T_i)^2} \left\{ \frac{2 Nu}{\sqrt{\pi}} - (1 - e^{Nu^2} erfc\ Nu) \right\} \qquad (II-3)$$

For Teflon, based on the values of its properties listed in Table I and the conditions under which the experiments were performed, the ratio given by Eq. (II-3) is approximately 0.75. Since the toal heat stored at this

time is in any case small compared with the total heat absorbed during the entire ablation process, this error is quite negligible (see Fig. 2 for comparison of the two profiles).

1. Ablation
2. Aerodynamic
   Heating
3. Boundary Layer
4. Axisymmetric Flow

I. Economos,
   Constantino
II. Wright Air
   Development
   Division
III. Contract AF
   33(616)-5944

Polytechnic Institute of Brooklyn
Aerodynamics Laboratory, Freeport, N. Y.
RESULTS OF ABLATION TESTS ON SEVERAL PLASTIC
MODELS IN A HYPERSONIC WIND TUNNEL.
by Constantino Economos. July 1961.
82pp. incl. figs. and tables. (Proj. 7364;
Task 73652) (PIBAL No. 606; WADD TN 60-273)
(Contract AF 33(616)-5944

Unclassified Report

An experimental study of transient ablation
has been carried out in a facility developed
expressly for this purpose. The facility
utilizes the PIBAL pebble bed convection
heater as a source of high energy air.
Hemispherical models made of several plastic
materials have been ablated and the final
configuration compared with the predictions
of a transient theory, which uses an integral

(over)

technique. Good agreement has been found
only for those plastics which sublime. For
the materials which melt and flow without
significant vaporization the transient theory
predicts values of the surface recession
which are much lower than those obtained ex-
perimentally. This discrepancy may be attri-
butable to unrealistic values of the phys-
ical properties available for these latter
materials.
The models were exposed to both a laminar
and transitional heat transfer environment.
The appropriate heat transfer theories re-
quired for the calculation are reviewed and
discussed in detail. Corresponding heating
rates have been measured experimentally and
are compared with these analyses. Theory
and experiment are shown to be in good
agreement.

1. Ablation
2. Aerodynamic Heating
3. Boundary Layer
4. Axisymmetric Flow

I. Economos, Constantino
II. Wright Air Development Division
III. Contract AF 33(616)-5944

Polytechnic Institute of Brooklyn
Aerodynamics Laboratory, Freeport, N.Y.
RESULTS OF ABLATION TESTS ON SEVERAL PLASTIC MODELS IN A HYPERSONIC WIND TUNNEL,
by Constantino Economos. July 1961.
82pp. incl. figs, and tables. (Proj. 7364; Task 73652) (PIBAL No. 606; WADD TN 60-273) (Contract AF 33(616)-5944

Unclassified Report

An experimental study of transient ablation has been carried out in a facility developed expressly for this purpose. The facility utilizes the PIBAL pebble bed convection heater as a source of high energy air.
Hemispherical models made of several plastic materials have been ablated and the final configuration compared with the predictions of a transient theory, which uses an integral

(over)

technique. Good agreement has been found only for those plastics which sublime. For the materials which melt and flow without significant vaporization the transient theory predicts values of the surface recession which are much lower than those obtained experimentally. This discrepancy may be attributable to unrealistic values of the physical properties available for these latter materials.
The models were exposed to both a laminar and transitional heat transfer environment. The appropriate heat transfer theories required for the calculation are reviewed and discussed in detail. Corresponding heating rates have been measured experimentally and are compared with these analyses. Theory and experiment are shown to be in good agreement.

UNCLASSIFIED

1. Ablation
2. Aerodynamic
   Heating
3. Boundary Layer
4. Axisymmetric Flow

I. Economos,
   Constantino
II. Wright Air
   Development
   Division
III. Contract AF
   33(616)-5944

UNCLASSIFIED

UNCLASSIFIED

Polytechnic Institute of Brooklyn
Aerodynamics Laboratory, Freeport, N. Y.
RESULTS OF ABLATION TESTS ON SEVERAL PLASTIC
MODELS IN A HYPERSONIC WIND TUNNEL.
by Constantino Economos. July 1961.
82pp. incl. figs. and tables. (Proj. 7364;
Task 73652) (PIBAL No. 606; WADD TN 60-273)
(Contract AF 33(616)-5944
                         Unclassified Report

An experimental study of transient ablation
has been carried out in a facility developed
expressly for this purpose. The facility
utilizes the PIBAL pebble bed convection
heater as a source of high energy air.
Hemispherical models made of several plastic
materials have been ablated and the final
configuration compared with the predictions
of a transient theory, which uses an integral
                                        (over)

technique. Good agreement has been found
only for those plastics which sublime. For
the materials which melt and flow without
significant vaporization the transient theory
predicts values of the surface recession
which are much lower than those obtained ex-
perimentally. This discrepancy may be attri-
butable to unrealistic values of the phys-
ical properties available for these latter
materials.

The models were exposed to both a laminar
and transitional heat transfer environment.
The appropriate heat transfer theories re-
quired for the calculation are reviewed and
discussed in detail. Corresponding heating
rates have been measured experimentally and
are compared with these analyses. Theory
and experiment are shown to be in good
agreement.

UNCLASSIFIED

Polytechnic Institute of Brooklyn
Aerodynamics Laboratory, Freeport, N. Y.
RESULTS OF ABLATION TESTS ON SEVERAL PLASTIC
MODELS IN A HYPERSONIC WIND TUNNEL.
by Constantino Economos. July 1961.
82pp. incl. figs, and tables. (Proj. 7364;
Task 73652) (PIBAL No. 606; WADD TN 60-273)
(Contract AF 33(616)-5944

Unclassified Report

An experimental study of transient ablation
has been carried out in a facility developed
expressly for this purpose. The facility
utilizes the PIBAL pebble bed convection
heater as a source of high energy air.
Hemispherical models made of several plastic
materials have been ablated and the final
configuration compared with the predictions
of a transient theory, which uses an integral

(over)

technique. Good agreement has been found
only for those plastics which sublime. For
the materials which melt and flow without
significant vaporization the transient theory
predicts values of the surface recession
which are much lower than those obtained ex-
perimentally. This discrepancy may be attri-
butable to unrealistic values of the phys-
ical properties available for these latter
materials.

The models were exposed to both a laminar
and transitional heat transfer environment.
The appropriate heat transfer theories re-
quired for the calculation are reviewed and
discussed in detail. Corresponding heating
rates have been measured experimentally and
are compared with these analyses. Theory
and experiment are shown to be in good
agreement.

Polytechnic Institute of Brooklyn
Aerodynamics Laboratory, Freeport, N. Y.
RESULTS OF ABLATION TESTS ON SEVERAL PLASTIC
MODELS IN A HYPERSONIC WIND TUNNEL.
by Constantino Economos. July 1961.
82pp. incl. figs, and tables. (Proj. 7364;
Task 73652) (PIBAL No. 606; WADD TN 60-273)
(Contract AF 33(616)-5944

Unclassified Report

An experimental study of transient ablation
has been carried out in a facility developed
expressly for this purpose. The facility
utilizes the PIBAL pebble bed convection
heater as a source of high energy air.
Hemispherical models made of several plastic
materials have been ablated and the final
configuration compared with the predictions
of a transient theory, which uses an integral

(over)

technique. Good agreement has been found
only for those plastics which sublime. For
the materials which melt and flow without
significant vaporization the transient theory
predicts values of the surface recession
which are much lower than those obtained ex-
perimentally. This discrepancy may be attri-
butable to unrealistic values of the phys-
ical properties available for these latter
materials.

The models were exposed to both a laminar
and transitional heat transfer environment.
The appropriate heat transfer theories re-
quired for the calculation are reviewed and
discussed in detail. Corresponding heating
rates have been measured experimentally and
are compared with these analyses. Theory
and experiment are shown to be in good
agreement.